

Article

Ketone Analog of Caffeic Acid Phenethyl Ester Exhibits Antioxidant Activity via Activation of ERK-Dependent Nrf2 Pathway

Khushwant S. Bhullar^{1,2,*}, Manal A. Nael^{3,4}, Khaled M. Elokely³ , Jérémie A. Doiron⁵, Luc M. LeBlanc⁵, Grégoire Lassalle-Claux⁵, Mohamed Salla⁶, Fahad S. Aldawsari⁷, Mohamed Touaibia⁵  and H. P. Vasantha Rupasinghe^{1,8} 

¹ Department of Plant, Food, and Environmental Sciences, Faculty of Agriculture, Dalhousie University, Truro, NS B2N 5E3, Canada; vrupasinghe@dal.ca

² Department of Pharmacology, Faculty of Medicine and Dentistry, University of Alberta, Edmonton, AB T6G 2H7, Canada

³ Institute for Computational Molecular Science and Department of Chemistry, Temple University, Philadelphia, PA 19122, USA; manal.nael@temple.edu (M.A.N.); kelokely@temple.edu (K.M.E.)

⁴ Department of Pharmaceutical Chemistry, Faculty of Pharmacy, Tanta 31527, Egypt

⁵ Department of Chemistry and Biochemistry, Université de Moncton, Moncton, NB E1A 3E9, Canada; jeremieadoiron@gmail.com (J.A.D.); LC280974@dal.ca (L.M.L.); lassalleclaux.gregoire@gmail.com (G.L.-C.); mohamed.touaibia@umoncton.ca (M.T.)

⁶ Department of Biochemistry, Faculty of Medicine and Dentistry, University of Alberta, Edmonton, AB T6G 2E1, Canada; salla@ualberta.ca

⁷ Reference Laboratory for Medicines and Cosmetics, Saudi Food and Drug Authority, Riyadh 2411, Saudi Arabia; fahad386@gmail.com

⁸ Department of Pathology, Faculty of Medicine, Dalhousie University, Halifax, NS B3H 4R2, Canada

* Correspondence: bhullar@ualberta.ca; Tel.: +1-780-492-3111



Citation: Bhullar, K.S.; Nael, M.A.; Elokely, K.M.; Doiron, J.A.; LeBlanc, L.M.; Lassalle-Claux, G.; Salla, M.; Aldawsari, F.S.; Touaibia, M.; Rupasinghe, H.P.V. Ketone Analog of Caffeic Acid Phenethyl Ester Exhibits Antioxidant Activity via Activation of ERK-Dependent Nrf2 Pathway. *Appl. Sci.* **2022**, *12*, 3062. <https://doi.org/10.3390/app12063062>

Academic Editor: Emanuel Vamanu

Received: 22 February 2022

Accepted: 11 March 2022

Published: 17 March 2022

Publisher's Note: MDPI stays neutral with regard to jurisdictional claims in published maps and institutional affiliations.



Copyright: © 2022 by the authors. Licensee MDPI, Basel, Switzerland. This article is an open access article distributed under the terms and conditions of the Creative Commons Attribution (CC BY) license (<https://creativecommons.org/licenses/by/4.0/>).

Abstract: Due to their robust antioxidant properties, phenolic acids and their analogs are extensively studied for their ability to activate cellular antioxidant pathways, including nuclear factor (erythroid-derived-2)-like 2 (Nrf2)-antioxidant response element (ARE) pathway. Caffeic, ferulic, and gallic acid are well-studied members of phenolic acids. Constant efforts are made to improve the pharmacological effects and bioavailability of phenolic acids by synthesizing their chemical derivatives. This study determines how modifications of the chemical structure of these phenolic acids affect their antioxidant and cytoprotective activities. We have selected six superior antioxidant compounds (**12**, **16**, **26**, **35**, **42**, and **44**) of the 48 caffeic acid phenethyl ester (CAPE) analogs based on their ability to scavenge free radicals in vitro using standard antioxidant assays. These compounds exhibited minimal toxicity as indicated by cell cycle and cytochrome C release assays. Among these compounds, **44**, the ketone analog of CAPE, exhibited the ability to increase p-Nrf2 (Ser40) levels in 293T cells ($p < 0.05$). Further, **44**, exhibited its antioxidant effect in *Drosophila Melanogaster* as indicated by an increase in mRNA levels of Nrf2 and GPx ($p < 0.05$). Finally, the ability of **44** to activate the antioxidant pathway was abolished in the presence of extracellular signal-regulated kinase (ERK) inhibitor in 293T cells. Thus, we identify **44**, the ketone analog of CAPE, as a unique antioxidant molecule with the function of ERK-mediated Nrf2 activation.

Keywords: caffeic acid; phenolic acid; antioxidant; oxidative stress; cell signaling

1. Introduction

In 1956, Harman presented the free radical theory, which suggested that the physiological damage triggered by free radicals was the prime determinant of aging [1]. The free radical theory was followed by the discovery of glutathione peroxidase (GPx) in 1957 and superoxide dismutase (SOD) in 1969, opening a new avenue for the study of antioxidants [2,3]. Miquel and colleagues (1980) further expanded the free radical theory with

mitochondria as the principal source and prime target of free radicals, creating a “vicious cycle” [4]. It was consolidated by the introduction of the concept of oxidative stress in 1985 which highlights that cellular damage is partly due to excess pro-oxidative factors over antioxidants [5]. The imbalance in metabolic sinks of pro- and anti-oxidants leads to redox alterations and cellular damage to carbohydrates, lipids, proteins, and DNA [6]. Among the free radical species, superoxide anion radical ($O_2^{\bullet-}$) and hydrogen peroxide (H_2O_2) play a vital role in oxidative damage [7]. Therefore, alleviation of oxidative stress and subsequent damage by increasing levels of endogenous antioxidants (GPx or SOD) is a rational approach.

In recent years, polyphenols of plant-based diet have gained tremendous interest as dietary antioxidants [8]. Chemically, polyphenols are compounds with at least one aromatic ring and one or more hydroxyl groups [9]. Among the structural chemistry of polyphenols, catechol moiety, in particular, has the ability to occupy delocalized unpaired electrons, which is one of the antioxidant activities [10,11]. Apart from the ability to directly scavenge free radicals, polyphenols act as signaling molecules to activate endogenous antioxidant pathways such as nuclear factor erythroid 2-related factor 2 (Nrf2) and its downstream targets [12]. By maintaining protective oxidoreductases and their nucleophilic substrates, the Nrf2 pathway boosts endogenous antioxidant enzymes [13]. During its activation, Nrf2 migrates from the cytoplasm into the nucleus, where it acts as a transcription factor and binds to the antioxidant response element (ARE) of genes involved in the antioxidant defense system, phase II drug detoxification, immunomodulation, and intracellular signaling [14]. Among its downstream effectors are SOD2 and GPx that can act as vital cytoprotective enzymes against oxidative stress. SOD2 protects cells by scavenging $O_2^{\bullet-}$, while GPx enzymes play a well-recognized role in H_2O_2 detoxification [15]. Therefore, the activation of these two enzymes presents a cogent strategy to tackle vital triggers of oxidative stress, i.e., $O_2^{\bullet-}$ and H_2O_2 . Multiple polyphenols activate the Nrf2 pathway and its downstream SOD2 and GPx enzymes [7,9]. In addition, the extracellular signal-regulated kinase (ERK) is an important upstream kinase that triggers the transcription of the Nrf2 pathway [16]. Multiple antioxidants such as erythropoietin, puerarin, luteolin, and sulfuretin elicit their pharmacological impact via activation of the Nrf2 pathway [17–20]. Among dietary antioxidants, phenolic acids, one of the major classes of polyphenols, have shown a strong ability to activate the Nrf2 pathway. Phenolic acids abundant in plant-based foods such as caffeic acid (CA), gallic acid (GA), and ferulic acid (FA) have all shown the ability to activate endogenous antioxidants [21–25]. However, guided by their chemistry and structure-function, new analogs of phenolic acids are continuously synthesized to improve their antioxidant ability and expand their pharmacological outcome.

Given the significant physiological importance of the Nrf2/ARE pathway, the identification of activators of this pathway has been a growing research interest. As a continuation of our previous work on phenolic acids [26], we compared the antiradical and antioxidant activity of recently reported phenolic acids-based 5-lipoxygenase inhibitors, to better understand their cytoprotective effects and the structure-activity relationship [27–31]. We also evaluated the effects of the chemical modifications on the basal cell cycle, cytotoxicity, antioxidant enzymes, oxidant cytokines, Nrf2, and associated pathway(s), in vitro and in vivo at basal conditions. The overall aim of the current study was to identify novel antioxidant(s) and potential activator(s) of the Nrf2 pathway in vitro and in vivo from multiple series of polyphenol analogs. Herein, based on our research goals, we present our findings highlighting the identification a unique antioxidant analog of caffeic acid phenethyl ester (CAPE) and show mechanisms underlying its antioxidant efficacy.

2. Materials and Methods

2.1. Synthesis of Compounds

Tested esters and ketones of phenolic acids were synthesized as previously reported [27–31]. Descriptions of the NMR analyzes of the seven selected compounds (1, 12, 16, 26, 35, 42, 44) after the first screening are as follows:

(E)-3-Phenylpropyl 3-(3,4-dihydroxyphenyl)acrylate (**1**) was synthesized according to the procedure that we previously reported [30]. The product was purified by flash chromatography; white solid; yield: 81%; ^1H NMR (400 MHz, DMSO- d_6) δ (ppm): 9.63 (br s, 1H, OH), 9.18 (br s, 1H, OH), 7.47 (d, J = 16 Hz, 1H, =CHC_{ar}), 7.29 (t, J = 7.4 Hz, 2H, H_{ar}), 7.24–7.17 (m, 3H, H_{ar}), 7.06 (s, 1H, H_{ar}), 7.02 (d, J = 9.1 Hz, 1H, H_{ar}), 6.77 (d, J = 8 Hz, 1H, H_{ar}), 6.28 (d, J = 16 Hz, 1H, =CHCO), 4.11 (t, J = 6.4 Hz, 2H, CH₂(CH₂)₂Ph), 2.68 (t, J = 7.44 Hz, 2H, (CH₂)₂CH₂Ph), 1.94 (quint., J = 6.8 Hz, 2H, CH₂CH₂CH₂Ph); ^{13}C NMR (101 MHz, DMSO- d_6) δ (ppm): 167.06, 148.85, 146.02, 145.55, 141.68, 128.81, 128.78, 126.33, 125.97, 121.84, 116.18, 115.29, 114.39, 63.58, 31.96, 30.36 (^1H and ^{13}C NMR spectra were included in the Supplementary Materials).

Phenethyl-2-(3,4-dihydroxyphenyl)acetate (**12**) was synthesized according to the procedure that we previously reported [29]. The product was purified by flash chromatography; yellow oil; yield: 63%; ^1H NMR (CD₃OD); δ (ppm): 7.27–7.14 (m, 5H, H_{ar}), 6.72–6.70 (m, 2H, H_{ar}), 6.54 (dd, J = 8.0 Hz, 1.7 Hz, 1H, H_{ar}), 4.27 (t, J = 6.8 Hz, CH₂CH₂Ph), 3.44 (s, 2H, C_{ar}CH₂CO), 2.89 (t, J = 6.8 Hz, 2H, CH₂CH₂Ph); ^{13}C -NMR (CD₃OD); δ (ppm): 172.56, 144.91, 144.06, 137.91, 128.59, 128.04, 126.05, 125.51, 120.28, 116.04, 114.92, 65.13, 40.14, 34.60 (^1H and ^{13}C NMR spectra were included in the Supplementary Materials).

Phenethyl 3,4,5-trihydroxybenzoate (**16**) was synthesized according to the procedure that we previously reported [31,32]. The product was purified by flash chromatography; white solid; yield: 67%; ^1H NMR (400 MHz, CDCl₃), δ (ppm): 7.36–7.26 (m, 7H), 4.51 (t, J = 7.0 Hz, 2H, CH₂CH₂Ph), 3.07 (t, J = 7.0 Hz, 2H, CH₂CH₂Ph). ^{13}C NMR (100 MHz, CDCl₃) δ (ppm): 166.48, 143.39, 137.74, 136.48, 128.94, 128.59, 126.65, 121.73, 65.75, 35.17 (^1H and ^{13}C NMR spectra were included in the Supplementary Materials).

3-(4-Methoxyphenyl)prop-2-yn-1-yl (2E)-3-[3,4-dihydroxyphenyl]prop-2-enoate (**26**) was synthesized according to the procedure that we previously reported [28]. The product was purified by flash chromatography; pale brown solid; yield: 96%; ^1H NMR (400 MHz, DMSO- d_6), δ (ppm): 9.50–9.20 (m, 2H, OH), 7.55 (d, 1H, J = 16 Hz, =CHC_{ar}), 7.41 (d, 2H, J = 8.6 Hz, H_{ar}), 7.09 (s, 1H, H_{ar}), 7.04 (d, 1H, J = 8.2 Hz, H_{ar}), 6.95 (d, 2H, J = 8.6 Hz, H_{ar}), 6.77 (d, 1H, J = 8.2 Hz, H_{ar}), 6.34 (d, 1H, J = 16 Hz, =CHCOO), 5.03 (s, 2H, CH₂CC), 3.78 (s, 3H, CH₃O). ^{13}C NMR (101 MHz, DMSO- d_6), δ (ppm): 166.40, 160.19, 149.13, 146.58, 146.04, 133.67, 125.84, 122.15, 116.18, 115.39, 114.83, 113.81, 113.52, 86.19, 83.39, 55.72, 52.70 (^1H and ^{13}C NMR spectra were included in the Supplementary Materials).

(2E)-3-(4-Methoxyphenyl)prop-2-en-1-yl (2E)-3-[3,4-dihydroxyphenyl]prop-2-enoate (**35**) was synthesized according to the procedure that we previously reported [28]. The product was purified by flash chromatography; pale yellow solid; yield: 91%; ^1H NMR (400 MHz, DMSO- d_6), δ (ppm): 7.52 (d, 1H, J = 16 Hz, =CHC_{ar}), 7.42 (d, 2H, J = 8.7 Hz, H_{ar}), 7.07 (d, 1H, J = 2.0 Hz, H_{ar}), 7.02 (dd, 1H, J = 8.2 Hz, 2.0 Hz, H_{ar}), 6.91 (d, 2H, J = 8.7 Hz, H_{ar}), 6.76 (d, 1H, J = 8.2 Hz, H_{ar}), 6.67 (d, 1H, J = 16 Hz, CH₂CH=CH), 6.33–6.24 (m, 2H, =CHCOO + CH₂CH=CH), 5.02 (s, 2H, OCH₂), 3.76 (s, 3H, OCH₃). ^{13}C NMR (101 MHz, DMSO- d_6), δ (ppm): 166.85, 159.62, 148.98, 146.05, 145.81, 133.56, 129.06, 128.31, 125.93, 121.96, 121.90, 116.19, 115.23, 114.55, 114.25, 64.96, 55.58 (^1H and ^{13}C NMR spectra were included in the Supplementary Materials).

(E)-3-(3,4-Dihydroxyphenyl)-1-phenylprop-2-en-1-one (**42**) was synthesized according to the procedure that we previously reported [28]. The product was purified by flash chromatography; yellow solid; yield: 99%; ^1H NMR (400 MHz, DMSO- d_6), δ (ppm): 9.45 (br s, 2H, OH), 8.10 (d, 2H, J = 7.6 Hz, H_{ar}), 7.67–7.54 (m, 5H, CH=CHCO + H_{ar}), 7.27 (s, 1H, H_{ar}), 7.19 (d, 1H, J = 8.1 Hz, H_{ar}), 6.82 (d, 1H, J = 8.1 Hz, H_{ar}). ^{13}C NMR (101 MHz, DMSO- d_6), δ (ppm): 189.45, 149.25, 146.08, 145.45, 138.49, 133.23, 129.19, 128.76, 126.71, 122.69, 118.87, 116.22, 116.01 (^1H and ^{13}C NMR spectra were included in the Supplementary Materials).

(E)-1-(3,4-Dihydroxyphenyl)-5-phenylpent-1-en-3-one (**44**) was synthesized according to the procedure that we previously reported [28]. The product was purified by flash chromatography; yellow solid; yield: 87%; ^1H NMR (400 MHz, Acetone- d_6), δ (ppm): 8.56 (br s, 1H, OH), 8.28 (br s, 1H, OH), 7.52 (d, 1H, J = 16.2 Hz, =CHC_{ar}), 7.31–7.28 (m, 4H, H_{ar}), 7.21–7.17 (m, 2H, H_{ar}), 7.07 (dd, 1H, J = 8.2 Hz, 2.0 Hz, H_{ar}), 6.88 (d, 1H, J = 8.2 Hz,

H_{ar}), 6.64 (d, 1H, J = 16.2 Hz, =CHCO), 2.99–2.97 (m, 4H, CH₂CH₂). ¹³C NMR (101 MHz, Acetone-d₆), δ (ppm): 198.13, 147.78, 145.31, 142.52, 141.79, 128.37, 128.27, 127.03, 125.79, 123.52, 121.89, 115.43, 114.30, 41.68, 29.95 (¹H and ¹³C NMR spectra were included in the Supplementary Materials).

2.2. Reagents

Dulbecco's Modified Eagle's Medium (DMEM), Eagle's Minimum Essential Medium (EMEM), fetal bovine serum (FBS), penicillin-streptomycin, 0.25% trypsin-EDTA, and PBS buffer were purchased from Gibco/Invitrogen (Carlsbad, CA, USA). Antibodies for Nrf2, p-Nrf2 (Ser40), AMPK, p-AMPK (Thr172) from Invitrogen (Carlsbad, CA, USA) were provided by Baksh lab, University of Alberta, Canada. SirT1 antibody (#2310, Cell Signaling Technology, Danvers, MA, USA) was provided by Hubbard lab, University of Alberta, Canada. Total extracellular signal-regulated kinase (ERK), p-ERK, HO-1, and GAPDH were obtained from Santa Cruz Biotechnology (Dallas, TX, USA). All the remaining reagents used in the study were purchased from Sigma-Aldrich (St. Louis, MO, USA).

2.3. Antioxidant Assays

Three antioxidant capacity assays were employed to assess the antioxidant activity of the phenolic acid(s) and their analogs in vitro. Ferric Reducing Ability of Plasma (FRAP) assay and Oxygen Radical Absorbance Capacity (ORAC) assays were performed as described in our previous report [33]. The 2, 2'-azino-bis-3-ethylbenzthiazoline-6-sulphonic acid (ABTS) was performed as described earlier [34]. The total antioxidant capacity of phenolic acid(s) and their analogs were expressed as μmol Trolox equivalents (TE)/L for the three assays.

2.4. Cell Culture

Human kidney epithelial HEK 293T cells (293T; ATCC[®] CRL-3216[™]) were obtained from the laboratory of Dr. Hasan Uludag, Chemical and Materials Engineering, University of Alberta, Canada, and cultured according to the supplier's instructions. These cells were maintained in DMEM supplemented with 10% fetal bovine serum (FBS) and 1% antibiotic/antimycotics in an atmosphere of 5% CO₂ at 37 °C. WI-38 (ATCC[®] CCL-75[™]) cells were obtained from ATCC (Baltimore, MD, USA) and cultured according to the supplier's instructions. These cells were maintained in EMEM supplemented with 10% fetal bovine serum (FBS) and 1% antibiotic/antimycotics in an atmosphere of 5% CO₂ at 37 °C. The cells were grown in 100 mm cell culture dishes or 6-well plates and treated with the indicated compounds or medium containing vehicle (DMSO) for 24 h. Following the treatment, cell lysates were collected using RIPA buffer.

2.5. Flow Cytometry Analysis

Cell cycle distribution was analyzed by measuring DNA content using a flow cytometer (FACS Canto II, BD Bioscience, CA, USA) with the Cell Cycle Kit (Beckman Coulter, Indianapolis, IN, USA). For the cell cycle analysis, 293T cells were grown in 6-well tissue culture plates until about 80% confluence and treated with the indicated compounds or medium containing vehicle (DMSO) for 24 h. Then, the cells were washed with PBS, trypsinized, and collected by centrifugation at 1000 × g for 5 min. Cell pellets were gently suspended in 400 μL PBS and 600 μL ice-cold 100% ethanol to fix. After storage at 4 °C for at least 3–4 h, the cells were collected again by centrifugation at 400 × g for 10 min. These cells were then incubated with 150 μL staining solution at 37 °C in the dark for 60 min before the analysis.

2.6. Antioxidant and Toxicity Analysis

Glutathione Peroxidase (GPx) assay kit (703102), NAD Cell-Based Assay Kit (600480), Interleukin-6 (human) ELISA Kit (501030), Tumor necrosis factor (TNF)-α (human) ELISA

Kit (589201) and Cytochrome c assay kit were obtained from Cayman Chemical (Ann Arbor, MI, USA). All assays were conducted according to the manufacturer's instructions.

2.7. Immunoblotting

The cells were grown in 6-well cell culture plates until they reached about 80% confluence, then treated with the indicated compounds, or medium containing vehicle (DMSO) for 24 h or treated with the indicated compounds along with ERK inhibitor SCH772984 (1 μ M) for 24 h. After incubation, the culture medium was removed, the cells were lysed in RIPA buffer and immunoblotting was performed.

2.8. *Drosophila Melanogaster* Study

To examine the effects of the selected phenolic acids on antioxidant enzymes *in vivo*, yellow white (*yw*) virgin mutant female flies (*D. melanogaster*) were used. All flies were reared, standard food and the feeding trials were conducted as described earlier [35]. Selected phenolic acids and their analogs were added to the molten fly-food media at 40–45 °C, stirred vigorously, and then agitated constantly while being poured in plastic tubes. The final concentration of the selected phenolic acids in the food was 10 μ M in the fly food. For the vehicle control, the equivalent carrier was added (DMSO). There were 50 flies in each treatment replicate ($n = 3$).

2.9. qPCR Analysis

Total RNA was isolated from flies by extraction with TRIzol reagent according to the manufacturer's instructions (Invitrogen, Waltham, MA, USA). cDNA was synthesized from 1 μ g total RNA using the reverse transcriptase (RT) system kit (Invitrogen, Waltham, MA, USA), and qPCR was performed using the CFX96 Touch Real-Time PCR Detection System (Biorad, Mississauga, ON, Canada).

2.10. Molecular Docking

The protein structural file of ERK2 in complex with caffeic acid (PDB ID: 4N0S was obtained from the RCSB Protein Data Bank [36]. Protein Preparation Wizard workflow was used to prepare the protein structure [37]. In the preprocessing stage, bond orders were assigned, missing hydrogen atoms were added, missing side chains and loops were filled in using prime [38–40]. Water molecules, beyond 5 Å from the ligand and that are not forming less than three hydrogen bonds to non-water residues, were deleted. In the final stage of protein preparation, hydrogen bonds were assigned after sampling water molecules, and the protein structure was subjected to restrained minimization allowing heavy atoms to converge to RMSD of 0.3 Å. A receptor grid was then generated by identifying the ligand coordinates (−15.26, 12.73, 40.72) to define the docking site. In order to add some flexibility to the docking process, the potential for nonpolar parts of the receptor was softened by scaling the van der Waals radii of receptor atoms that have a partial charge cutoff of 0.25, with a scaling factor of 0.8. All hydroxyl and thiol groups of the amino acids in the receptor grid were allowed to rotate during the docking process. Ligand structures were sketched in maestro using OPLS3 forcefield and prepared with LigPrep [41,42]. Possible ionization and tautomerization states were generated at pH 7.4. The lowest energy conformer was kept for each ligand. Molecular docking was performed using a Glide standard precision approach [43–45]. CA was docked to validate the docking protocol, and the crystallized binding mode was retrieved from the best pose. Five poses per ligand were written in the pose viewer file. The docking results were then refined by running Prime MM-GBSA calculation [38,39]. Amino acid residues within 10 Å of the ligand are allowed to be flexible during the optimization step.

2.11. Metabolism Prediction

Prediction of metabolic fate of selected analogs of phenolic acids was conducted as described in a recent report [46]. Among key results, the polar surface area was presented

as topological polar surface area (TPSA), iLOGP (for implicit log P) was calculated based on Gibbs free energy of solvation, skin permeability coefficient ($\log K_p$ in cm/s), bioavailability score (probability of 10% oral bioavailability), and synthetic accessibility score, indicating the ease of synthesis, are presented.

2.12. Statistical Analysis

All the data are presented as mean \pm SEM of three independent experiments. Data were analyzed by one-way analysis of variance (ANOVA) with Dunnett's test for comparisons to the vehicle using PRISM 7 statistical software (GraphPad Software, San Diego, CA, USA). $p < 0.05$ was considered to be statistically significant.

3. Results

3.1. Phenolic Acids and Their Analogs Exhibit Robust Antioxidant Activity

Three antioxidant assays, FRAP, ORAC, and ABTS were employed to measure the antioxidant potential of the compounds of the five series as well as the standards (see the Supplementary Data). The selection of the potent compound(s) from each series was based on the cumulative antioxidant activity based on the three assays. Supplementary Information has been added indicating the detailed antioxidant values of all compounds in the three assays (Figure S1A–F and Table S1A–F). Herein, we report the summary of the antioxidant activity of selected efficacious compounds. Among analogs of series 1, ester **12**, the phenyl acetic acid analog of CAPE, exhibited the strongest antioxidant activity among the tested compounds ($p < 0.01$) in vitro (Figure 1A). It exhibited FRAP, ORAC, and ABTS values of 374 ± 9.2 , 421 ± 11.3 , and 523 ± 0.4 $\mu\text{mol TE/L}$ (Figure S1A and Table S1A). Ester **16**, the CAPE's analog, exhibited the strongest antioxidant activity (Figure 1B) with FRAP, ORAC, and ABTS values of 315 ± 6.5 , 336 ± 2.1 , and 523 ± 1.3 $\mu\text{mol TE/L}$, respectively, among the related analogs of series 2 ($p < 0.05$) in vitro (Figure S1B and Table S1B). Further, in series 3 and 4, esters **26** and **35** exhibited the strong ability to quench free radicals ($p < 0.05$) in vitro (Figure 1C,D). Bearing 3-phenylpropargyl (**26**) and 3-phenylallyl (**35**) moieties, esters **26** and **35** are less flexible compared to CAPE or ester **1**. Their antioxidant capacity as indicated by the FRAP, ORAC, and ABTS was 288 ± 2.7 , 226 ± 8.4 , 486 ± 4.4 and 303 ± 6.6 , 459 ± 15.3 , and 510 ± 18.1 $\mu\text{mol TE/L}$, respectively (Figure S1C and Table S1C). Finally, in series 5, 3,4-dihydroxychalcone **42** and its related phenethyl analog **44** exhibited a stronger activity in comparison to the other analogs ($p < 0.05$) in vitro (Figure 1E). Their antioxidant capacity as indicated by the FRAP, ORAC, and ABTS was 222 ± 13.8 , 444 ± 1.1 and 511 ± 1.0 and 231 ± 3.5 , 438 ± 2.8 , 517 ± 6.4 $\mu\text{mol TE/L}$, respectively (Figure S1E and Table S1E). The modification of the caffeic acid moiety as well as the replacement of the ester functional group by an ether did not have a significant effect on the antioxidant activity. None of the compounds in series 2 and 6 exhibited consistent and strong activity in the three assessment assays conducted in vitro (Figure 1B,F; Table S1B,F). The extensive antioxidant analysis using multiple assays revealed robust antioxidant activities of phenolic acid derivatives in vitro (Figure 1A–F, Table S1A–F).

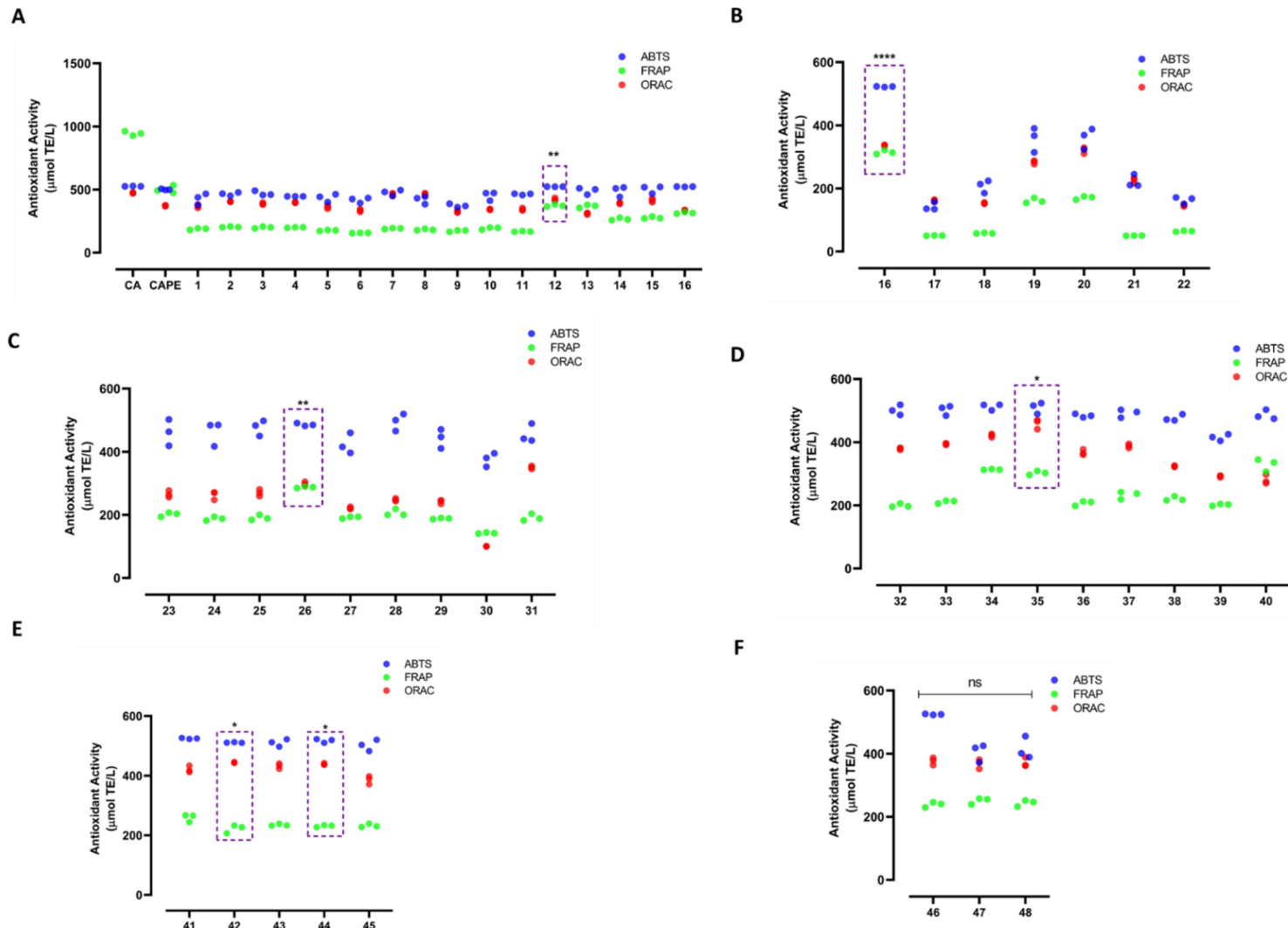


Figure 1. Antioxidant activity of Caffeic acid and CAPE analogs (100 μM) as measured using ABTS, FRAP, and ORAC antioxidant assays. Selective compounds from each series of analogs (A–F) with significant antioxidant activities were selected for further studies following statistical analysis. * $p < 0.05$, ** $p < 0.01$, **** $p < 0.0001$, ns: non-significant.

3.2. Selected Phenolic Acid Analogs Exhibit Minimal Toxicity

After selecting the potent analogs, based on their antioxidant activity (Figure 2A–I), they were assessed for their toxicity in 293T cells *in vitro*. Two assays, cell cycle analysis using PI and cytochrome C release assay were conducted to investigate the toxicity and cell injury induced by these compounds at the tested concentration (10 μ M) for 24 h. The PI-stained whole cells following treatment with the selected compounds exhibited minimal toxicity in 293T cells *in vitro* (Figure 3A–J). As shown in the condensed heatmap (Figure 3K), the percentage of the cells in the G1, S, and G2 phase(s) remained statistically unchanged, indicating the low toxicity of selected compounds as compared to the vehicle (Figure 3K). None of the compounds induced G1-phase arrest and downstream apoptosis in 293T cells *in vitro*. Likewise, the assessed cytochrome C levels indicate no increase in apoptosis in WI-38 cells *in vitro* by the caffeic acid and its derivatives (Figure S2). However, one of the selected compounds, ketone **42**, increased the cytochrome C levels by an average of 1.5 fold in WI-38 cells *in vitro* (Figure S2). Low toxicity in both the cell lines, 293T and WI-38, being normal (non-cancerous) epithelial and fibroblast cells endorse the further pharmacological investigation of the selected non-toxic antioxidant compounds in both cells and *in vivo* models.

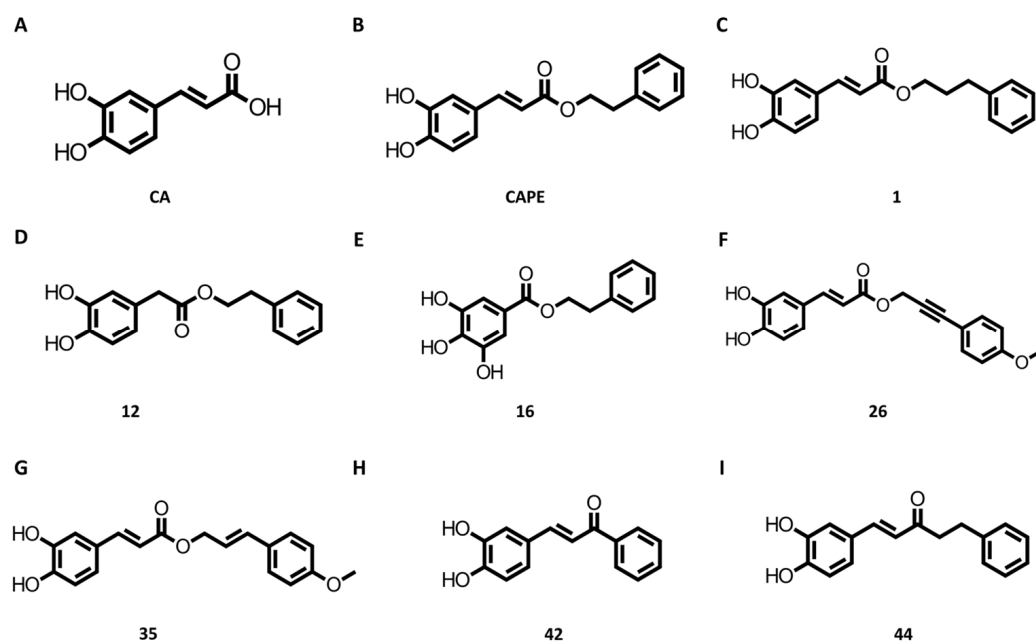


Figure 2. Chemical structures (A–I) of key antioxidant esters and ketones of selected phenolic acids.

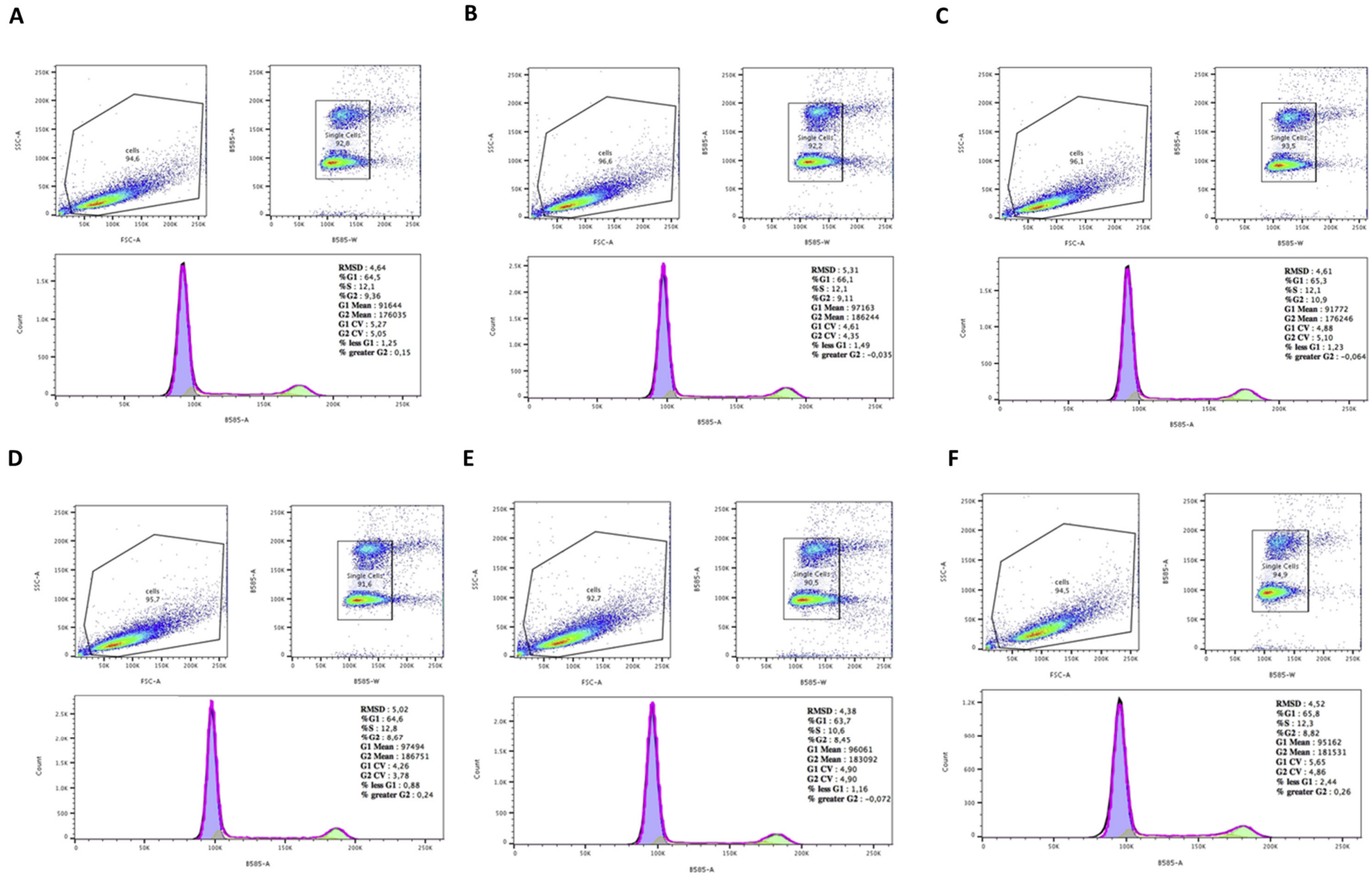


Figure 3. Cont.

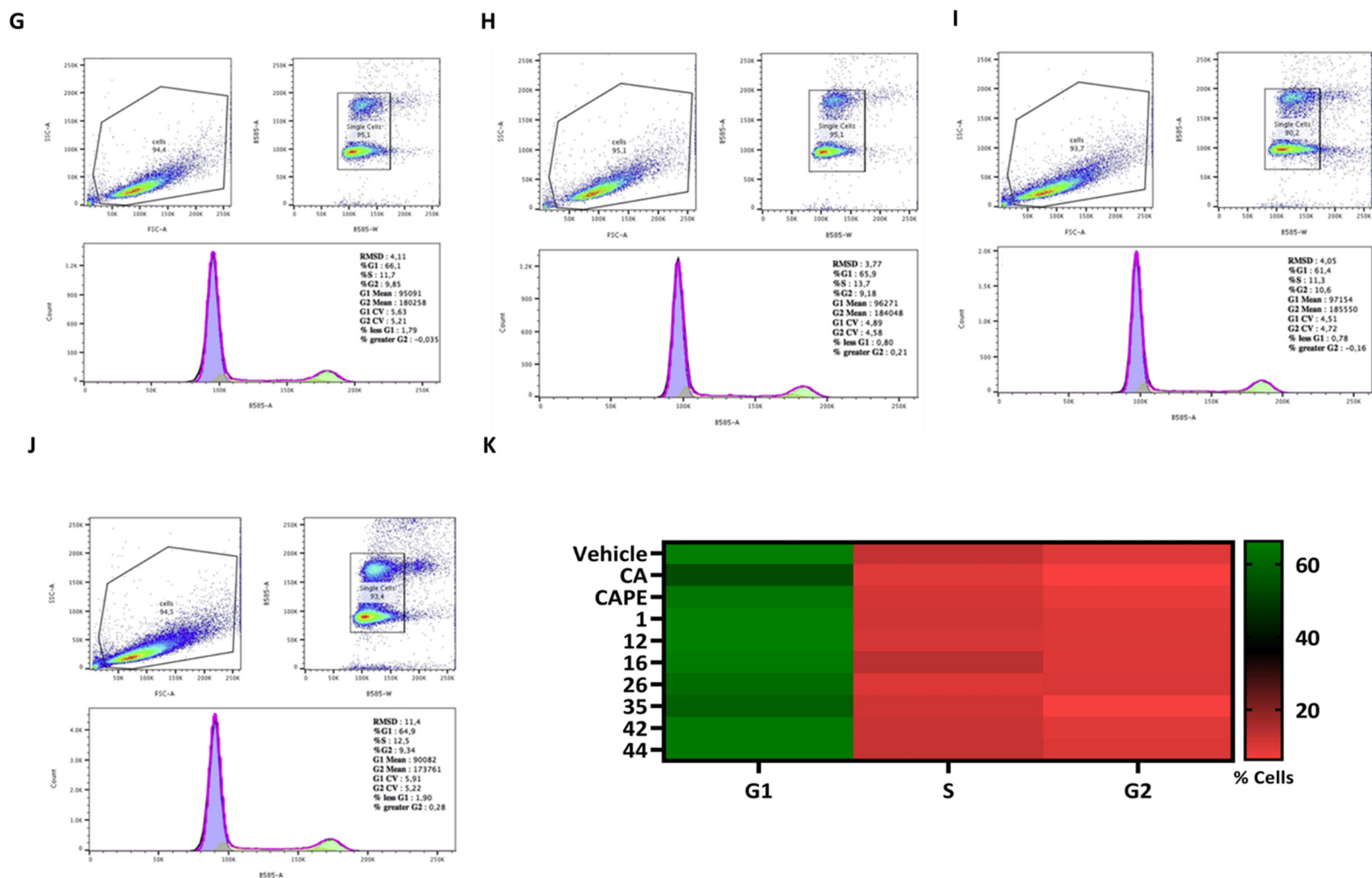


Figure 3. The impact of Caffeic acid and CAPE analogs on the cell cycle as the toxicity indicator. The 293T cells were pre-treated with 10 μ M of the selected compounds for 24 h and the cell cycle was analyzed using propidium iodide (A) Vehicle, (B–J) impact of CA and CAPE pre-treatment on AAPH induced oxidative insult, and (K) the graphical representation of the trend in the cell cycle of 293T cells in response to different treatments.

3.3. Selected Phenolic Acid Analogs Increase GPx and Lower TNF α Levels

The selected non-toxic antioxidant compounds were then assessed for their ability to stimulate antioxidant enzymes, NAD pool, and possibly lower oxidative stress markers such as IL-6 and TNF α . We selected these biomarkers owing to the close interaction between oxidative damage and antioxidant enzymes, energy metabolism, and immune activation. Our ELISA results showed that compared to the vehicle, all tested compounds, except ester **12**, activated GPx, a selenium-containing functional antioxidant enzyme (Figure 4A). The relatively lower antioxidant activity was exhibited by ketone **42** ($p < 0.001$); while the remaining compounds exhibited higher antioxidant activity ($p < 0.0001$) compared to the vehicle in 293T cells in vitro. Considering their nontoxic nature, the robust increase in the GPx levels indicate the strong ability of selected compounds to catalyze the reduction of hydroperoxides, including H₂O₂ and related free radicals, to protect the cell from oxidative damage. We also inquired to see if these compounds can boost NAD pool levels as NAD⁺ (oxidized form) and NADH (reduced form) are the core components in redox reactions. Our results showed that none of the tested compounds increased the total NAD pool levels in 293T cells in vitro (Figure 4B). Interestingly, CA, **16**, and **42** boosted levels of SIRT1, an NAD⁺-dependent deacetylase (Figure S3). Contrarily, CAPE, **1**, **26**, and **35** lowered the levels of SIRT1 compared to the vehicle in 293T cells in vitro (Figure S3). Next, we investigated if the selected compounds can lower cellular cytokines IL-6 and TNF α , known to perturb the redox signaling cascade. Our ELISA results showed that most of the compounds had no impact on basal levels of IL-6, except CAPE, which increased its levels ($p < 0.05$) (Figure 4C). However, CA, CAPE, and **1** increased the TNF α levels in cells (Figure 4D). However, the fold change increase in TNF α was below 1.5-fold in all the compounds and was statistically significant. Interestingly, CAPE induces both cytokines IL-6 and TNF α in 293T cells in vitro (Figure 4C,D). These cytokine-promoting compounds may induce mild stress in the cells and trigger an antioxidant response. Further, ketones **42** ($p < 0.0001$) and **44** ($p < 0.01$) significantly reduced the TNF α levels in cells in vitro (Figure 4D). These ELISA analyses show that various phenolic acid analogs boosted the levels of antioxidant enzyme GPx in cells, possibly by inducing xenohormesis stress response in a NAD pathway independent manner.

3.4. Selected Phenolic Acid Analogs Activate the Nrf2 Pathway in Cells

Next, we assessed if the selected phenolic acid analogs can initiate the Nrf2 pathway, the major regulator of antioxidant responses in cells. Interestingly, many phenolic acids and their analogs initiated phosphorylation of Nrf2 (Ser40) under basal conditions in 293T cells in vitro. Among the tested compounds, CA, CAPE, **1**, and **44** significantly increased the phosphorylation of Nrf2 (Ser40) in 293T cells in vitro (Figure 5A). The activity of compound **44** was validated independently as well (Figure S4C). Likewise, the increased mRNA levels of Nrf2 were supportive of the Nrf2 pathway activation (Figure 5B). Interestingly, the compounds stimulating mild stress, induced phosphorylation of Nrf2 (Ser40) in 293T cells in vitro (Figures 4C and 5A,B). The Nrf2 phosphorylating compounds initiated the ERK and downstream HO-1 pathway as well (Figure 5C,D). The three potent in vitro antioxidants **16**, **26**, and **35** failed to improve the levels of Nrf2 in 293T cells in vitro (Figure 5A,B). It is possible that these compounds can quench the free radicals directly without the activation of the antioxidant pathways. In addition, CAPE emerged as the strongest ERK activator (p-ERK Thr204) in 293T cells in vitro (Figure 5C). However, the results from HO-1 activation were contradictory between mRNA and protein analysis as the compounds exhibiting high mRNA levels of HO-1 were weak at the protein expression and vice-versa (Figures 5D and S4A,B).

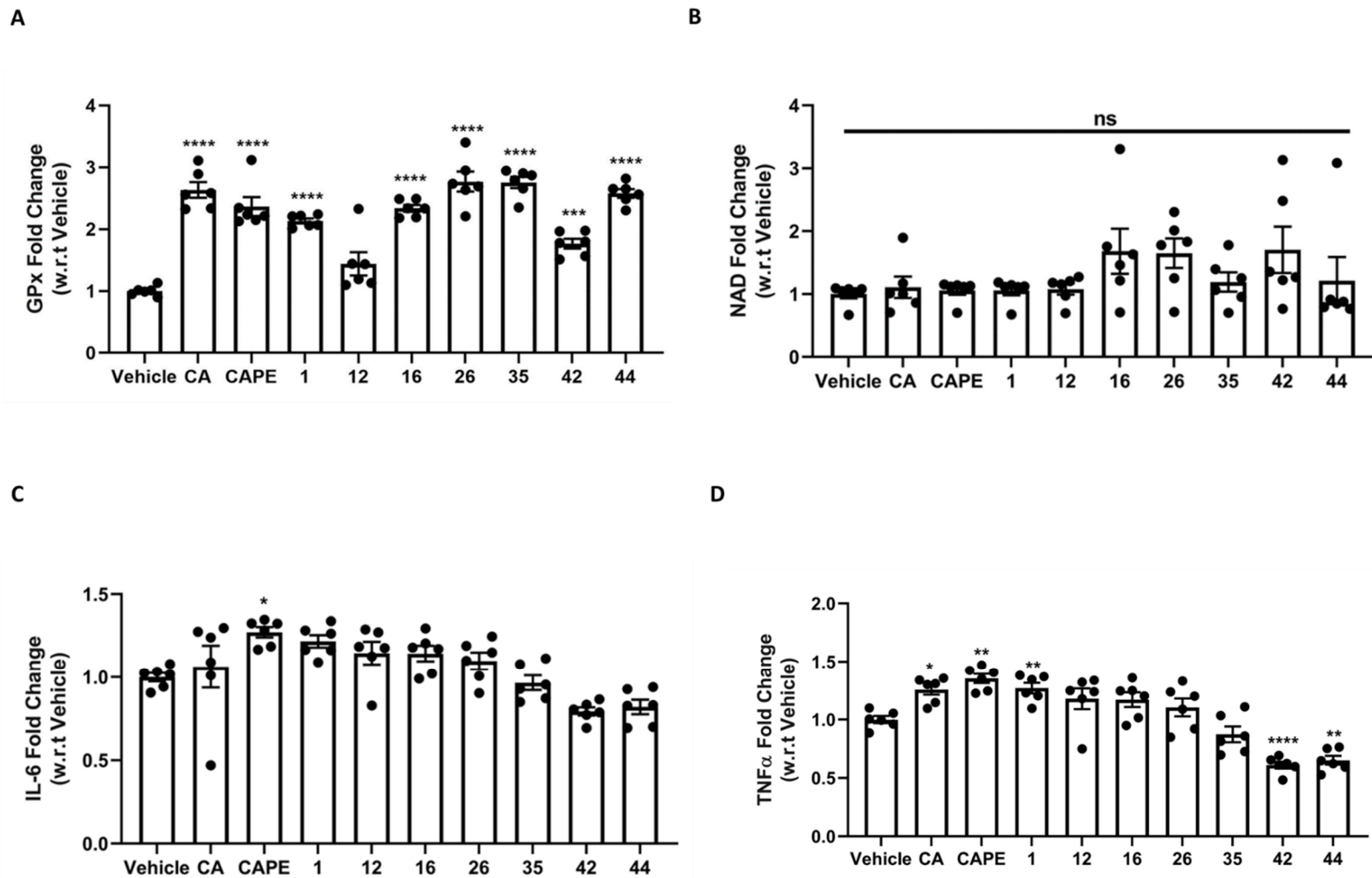


Figure 4. The impact of Caffeic acid and CAPE analogs on various antioxidant parameters. The 293T cells were pre-treated with 10 μ M of the selected compounds for 24 h and then the selected biomarkers were observed using ELISA: (A) GPx (B) NAD (C) IL-6 and (D) TNF α were analyzed. Ordinary one-way analysis of variance (ANOVA) was performed followed by Dunnett’s multiple comparisons test to identify statistical difference * $p < 0.05$, ** $p < 0.01$ *** $p < 0.001$, **** $p < 0.0001$, ns: non-significant.

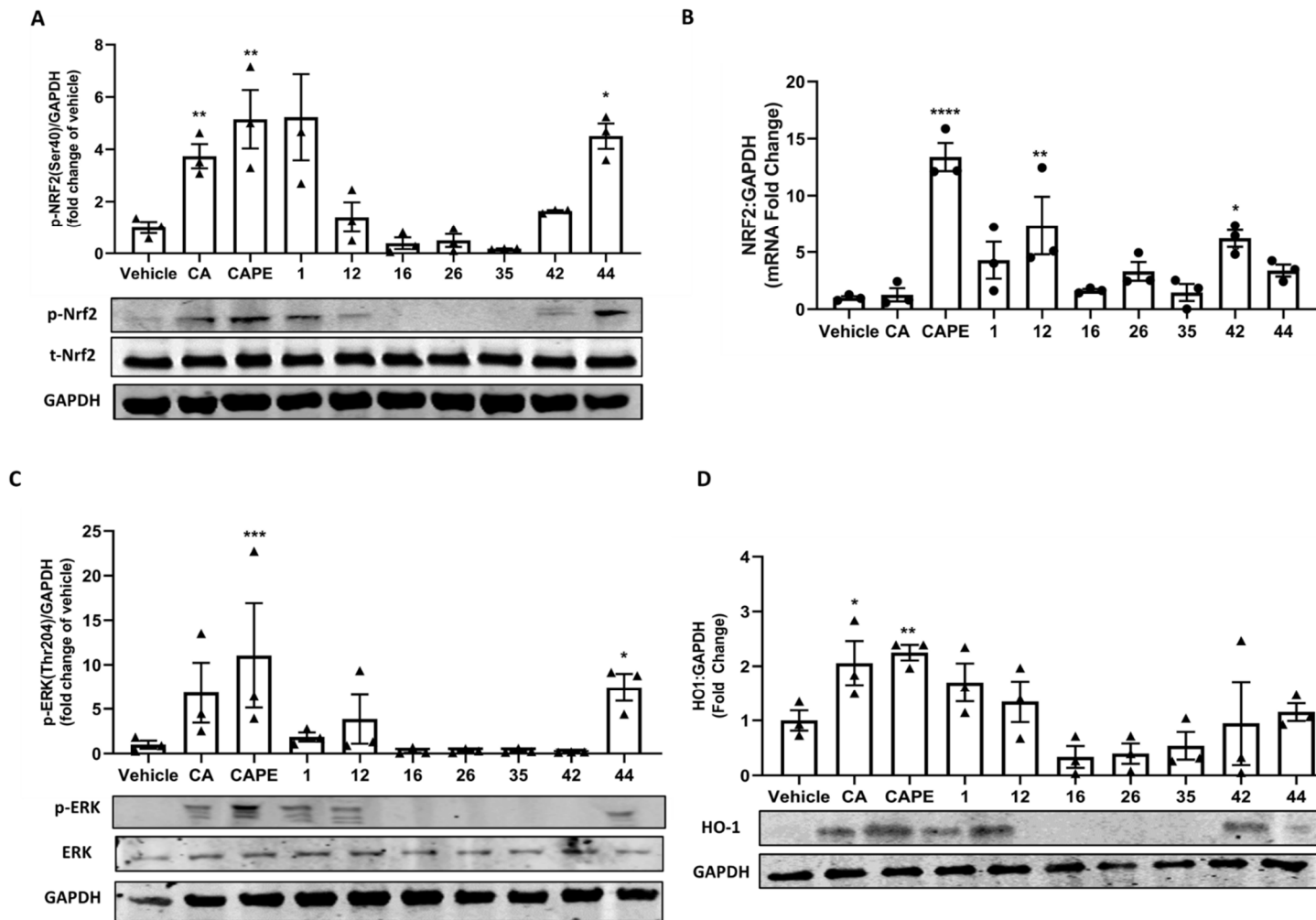


Figure 5. The impact of Caffeic acid and CAPE analogs on Nrf2 pathway activation. The 293T cells were pre-treated with 10 μ M of the selected compounds for 24 h and then the protein and RNA were extracted using RIPA buffer and TRIzol. (A) Changes in p-Nrf2(Ser40) ratio (B) Nrf2 mRNA increase (C) changes in ratio of p-ERK (Thr204) ratio and (D) HO-1 were analyzed. Ordinary one-way analysis of variance (ANOVA) was performed followed by Dunnett’s multiple comparisons test to identify statistical difference * $p < 0.05$, ** $p < 0.01$, *** $p < 0.001$, **** $p < 0.0001$.

3.5. Selected Phenolic Acid Analogs Activate the Nrf2 Pathway in *D. melanogaster*

Following the assessment of the antioxidant activity in situ and cells, we employed *D. melanogaster* for in vivo analysis of the selected polyphenols. The virgin yellow white (*yw*) mutant female flies used in the current study were fed the selected compounds for 2 weeks (10 μ M) (Figure 6A). The qPCR analysis showed a strong increase in Nrf2 and downstream GPx antioxidant enzyme expression in *yw* flies in vivo (Figure 6B,C). Similar to the cell study, CA, CAPE, **1**, and **44** significantly initiated Nrf2 activation (Figures 5B and 6B). Likewise, strong GPx stimulation was induced by most compounds with a statistically significant increase by CAPE and **44** in *yw* flies in vivo (Figures 4A and 6C). However, no significant increase in SOD levels was noticed in *yw* flies in vivo (Figure 6D). The *Drosophila* studies confirm the pattern of antioxidant and cytoprotective activity of the selected phenolic acid derivatives in vivo (Figure 6). The in vivo results along with the cell studies present J198, the CAPE's ketone analog, as a unique activator of the Nrf2 pathway both in vitro and in vivo.

3.6. Antioxidant Activity of Selected Phenolic Acid Analogs Is ERK-Dependent

Next, owing to the dynamic role of ERK in Nrf2 pathway activation, we investigated if the antioxidant activity of selected compounds in ERK-dependent using an ERK inhibitory model in vitro (Figure 7A). Similar to the ELISA study (Figure 4A), immunoblotting showed that the selected phenolic acid and their analogs (CA, CAPE, **1**, **12**, and **44**) stimulated the GPx expression in 293T cells in vitro (Figure 7B). Our results confirmed the hypothesis as the increased expression of GPx by these compounds was inhibited following co-treatment with ERK inhibitor (1 μ M, SCH772984) in 293T cells in vitro (Figure 7C). These results indicate the essential role of ERK in the chain of cell communication by selected phenolic acids from a receptor to protein expression.

3.7. Selected Phenolic Acid Analogs Interact with the Active Site of ERK

The binding modes of the analogs were predicted in ERK using caffeic acid as the reference frame. CA was crystallized in complex with ERK2. It interacts with the hinge region amino acids; Gln105, Asp106, and Met108 through hydrogen bonds through the phenolic hydroxyl groups. The carboxylate group demonstrated an ionic interaction with Lys54. The atomic coordinates of CA were used to define the docking site for the phenolic acid analogs. In order to better understand the binding affinity of each analog, the binding free energy of the receptor and ligand was calculated using the implicit solvent method. Analogs **12**, **16**, **26**, **35**, **42**, and **44** showed a perfect fit in the binding pocket of ERK2. The phenolic ring of these analogs aligned well with that of CA (Figure 8A panel I). Similar interactions with the hinge region were observed as well. The terminal phenyl group of **12**, **16**, **42**, and **44** occupies the solvent-accessible area of the binding site (Figure 8B). There is no loss in solvation/desolvation energy, which can explain in part the high affinity of these analogs. The binding free energy (-40 to -50 kcal/mol) of these analogs also suggests high binding.

3.8. Selected Phenolic Acid Analogs Exhibit Stronger Metabolic Uptake

The metabolic simulation studies supported our findings on the antioxidant activities of selected polyphenol analogs (Figure 9). All selected compounds exhibited TPSA between a healthy range of 20 and 130 \AA . Most analogs exhibited lower TPSA, thus aiding their polarity and ability to cross the biological barriers for absorption. Ketones **42** and **44** exhibited the lowest TPSA backed by high GI and brain availability (Figure 9). However, the skin permeability coefficient ($\log K_p$ in cm/s) and bioavailability score of analyzed compounds were similar (Figure 9). Overall, when calculations were completed, the "BOILED-Egg" analysis confirmed the high bioavailability of analogs compared to the parent molecules in both GI and BBB settings (Figure 9).

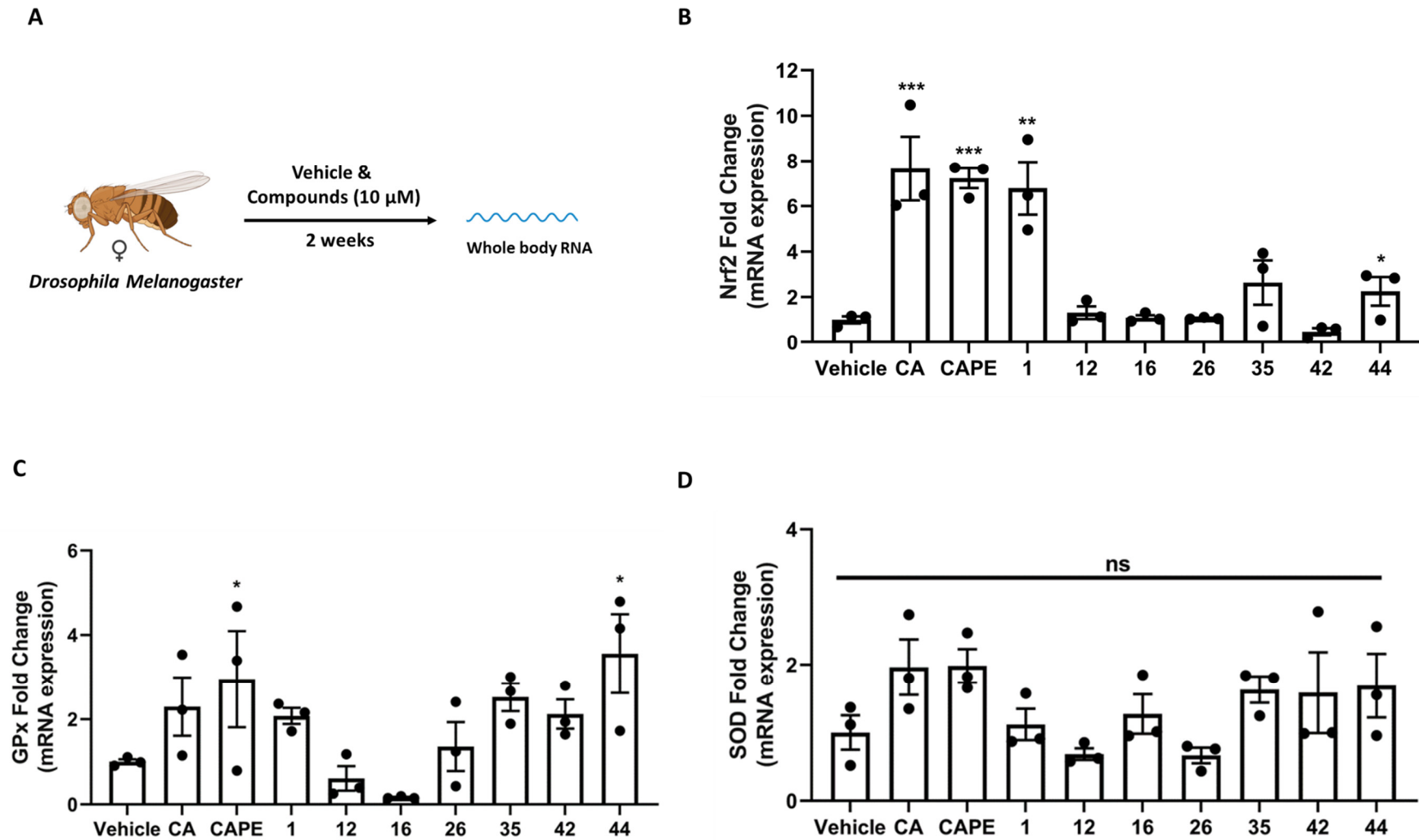


Figure 6. The impact of Caffeic acid and CAPE analogs on Nrf2 pathway activation in *Drosophila Melanogaster*. (A) The virgin yellow white (*yw*) mutant female flies were fed the selected compounds for 2 weeks (10 μ M) and then the total RNA was extracted using TRIzol. Changes in (B) Nrf2 (C) GPx (D) SOD mRNA levels were analyzed. Ordinary one-way analysis of variance (ANOVA) was performed followed by Dunnett’s multiple comparisons test to identify statistical difference * $p < 0.05$, ** $p < 0.01$, *** $p < 0.001$, ns: non-significant.

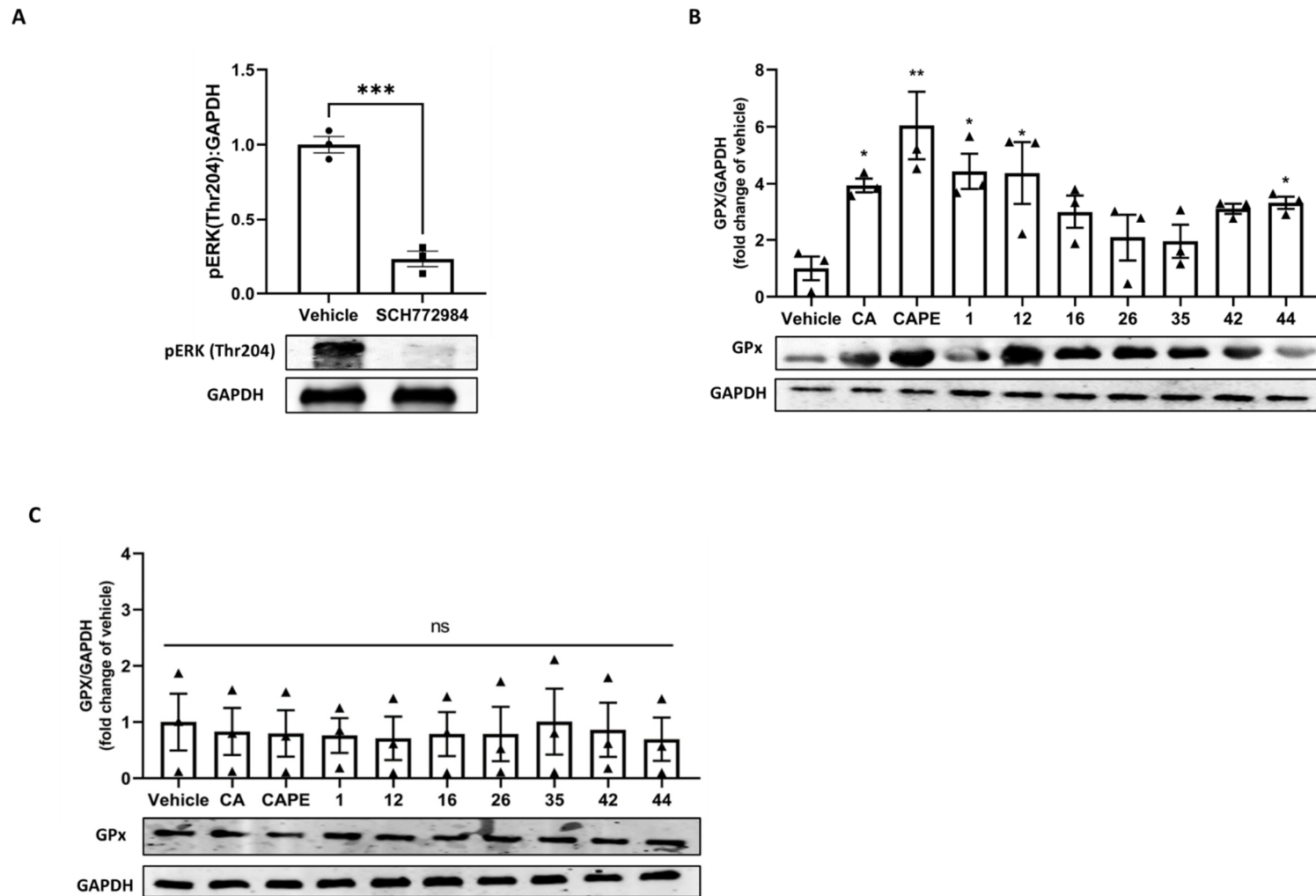


Figure 7. The impact of Caffeic acid and CAPE analogs on key antioxidant parameter GPx is dependent on ERK phosphorylation. (A) ERK inhibitor SCH772984 (1 μ M) was used to lower ERK phosphorylation levels in 293T cells (immunoprecipitated). Next, 293T cells were pre-treated with 10 μ M of the selected compounds for 24 h, (B) without and (C) with ERK inhibitor SCH772984 (1 μ M), and then the changes in selected biomarker, GPx, was observed using western blot. * $p < 0.05$, ** $p < 0.01$, *** $p < 0.001$, ns: non-significant.

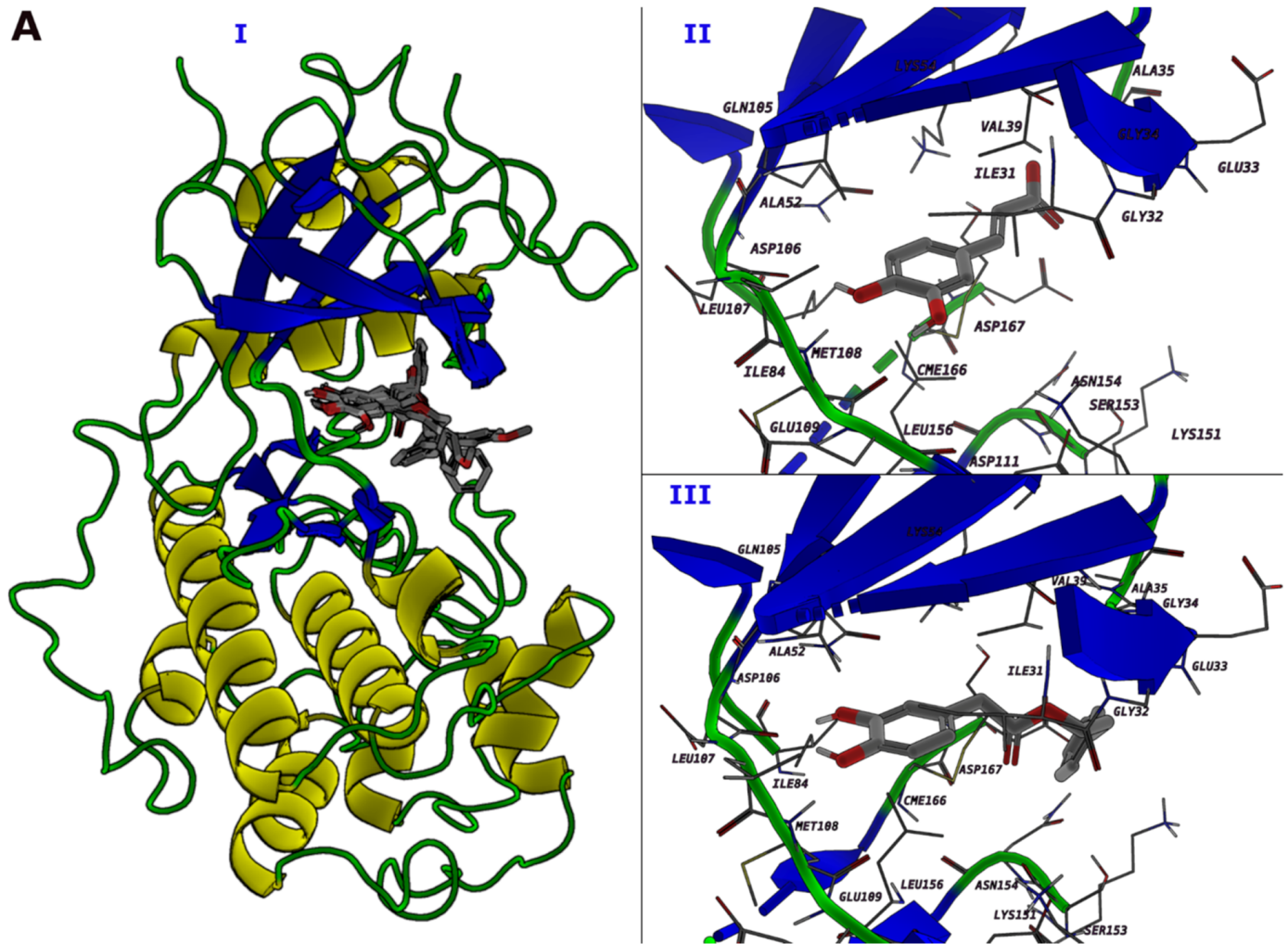


Figure 8. Cont.

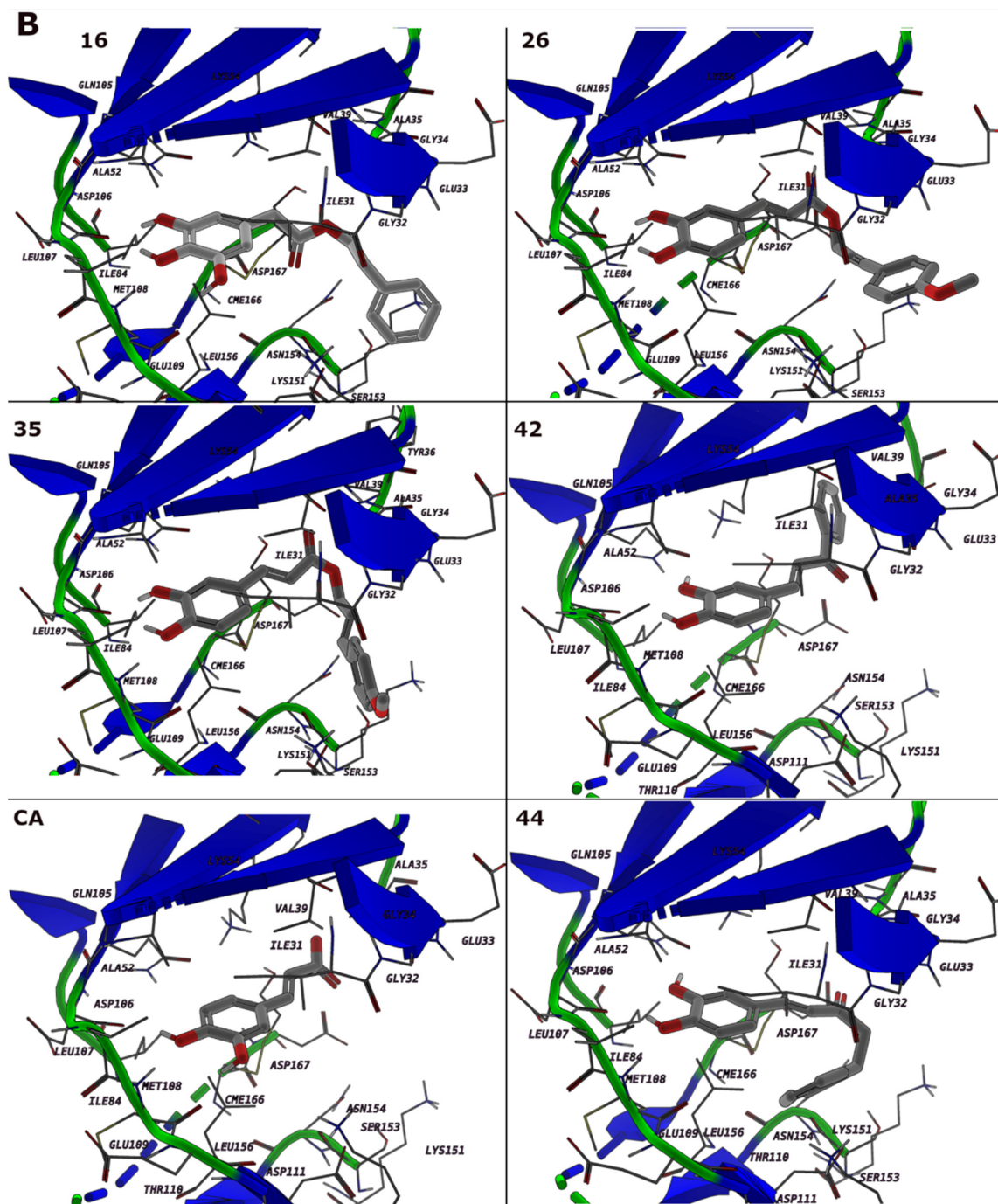
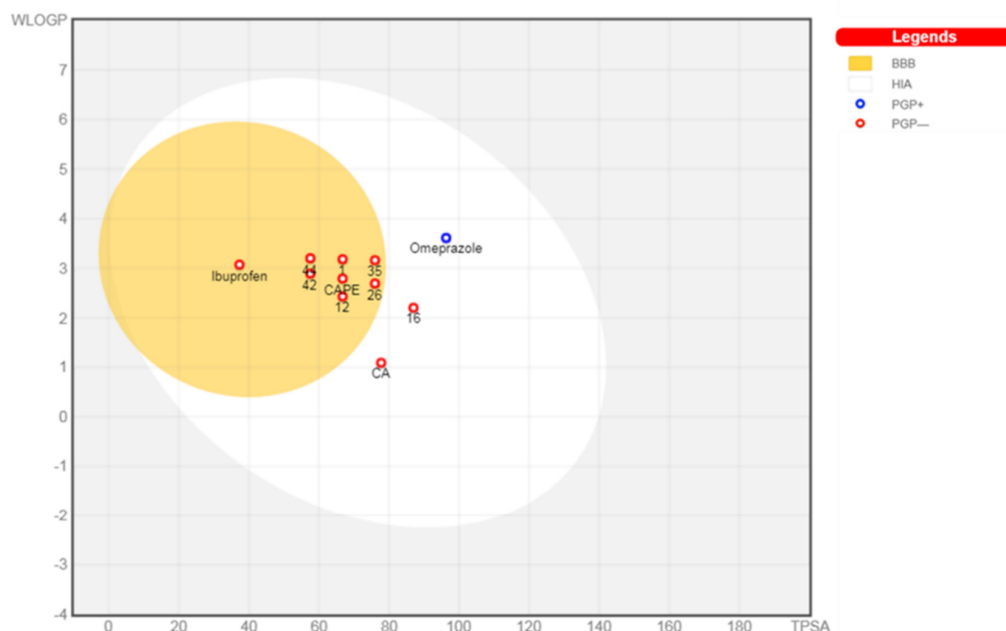


Figure 8. The interaction of selected analogs of phenolic acids with ERK depicted by molecular docking. (A). The binding modes of the phenolic acid analogs. I. Alignment of selected analogs in the active site of ERK2. II. Caffeic acid interaction model. III. Analog 12 interaction model. The protein is shown as cartoon, ligand as sticks, and the interacting amino acids as lines. (B). The interaction models of selected phenolic acid analogs; 16, 26, 35, 42, Caffeic acid, and 44. The protein is shown as cartoon, ligand as sticks, and the interacting amino acids as lines. Caffeic acid is given as the reference frame for comparison. Caffeic acid interacts through HB with Asp106 and Met108. It shows electrostatic contacts with Lys54, Gln105, Asp106 and Lys114. It exerts several hydrophobic contacts with Ile31, Gly34, Ala35, Val39, Ala52, Ile84, Leu107, Met108 and Leu156. Compound 12 exhibits these types of interactions with the surrounding amino acids; hydrogen bonds with Gln105, Asp106, and Met108, electrostatic type with Glu33, Lys54, Gln105, Asp106, Asp111, Lys114, Lys151, Asn154, Ser153, and Asp167, and hydrophobic contacts with Ile31, Gly34, Ala35, Val39, Ala52, Ile84, Leu107,

Met108, and Leu156. Compound 26 interacts with Gln105, Asp106, and Met108 by hydrogen bonds. The polar amino acids Glu33, Lys54, Gln105, Asp106, Asp111, Lys114, and Ser153 interact electrostatically with compound 26. The hydrophobic contacts involve Tyr30, Ile31, Gly32, Gly34, Val39, Ala52, Ile84, Leu107, Met108, and Leu156. Compound 35 Interacts with the surrounding amino acids via these types of interactions; hydrogen bonds with Ala35, Asp106, and Met108, electrostatic interactions with Glu33, Lys54, Gln105, Asp106, Asp111, Lys114, and Ser153, and hydrophobic contacts with Ile31, Gly32, Gly34, Ala35, Val39, Ala52, Ile84, Leu107, Met108, and Leu156. Compound 42 Interacts with the surrounding amino acids via these types of interactions; hydrogen bonds with Gln105, Asp106, and Met108, electrostatic interactions with Lys54, Lys55, Gln105, and Asp106, and hydrophobic contacts with Ile31, Ala35, Tyr36, Val39, Ala52, Ile56, Ile84, Leu107, Met108, and Leu156. Compound 44 Interacts with the surrounding amino acids via these types of interactions; hydrogen bonds with Gln105, Asp106, and Met108, electrostatic interactions with Glu33, Lys54, Gln105, Asp106, Glu109, Thr110, Asp111, Lys114, and Ser153, and hydrophobic contacts with Ile31, Gly32, Gly34, Val39, Ala52, Ile84, Leu107, Met108, and Leu156.



Molecule	TPSA	iLOGP	GI absorption	BBB permeant	log Kp (cm/s)	Bioavailability Score	Synthetic Accessibility
CA	77.76	0.97	High	No	-6.58	0.56	1.81
CAPE	66.76	2.66	High	Yes	-5.09	0.55	2.64
1	66.76	2.86	High	Yes	-4.86	0.55	2.63
12	66.76	2.07	High	Yes	-5.65	0.55	2.08
16	86.99	1.83	High	No	-5.92	0.55	2.19
26	75.99	3.27	High	Yes	-5.91	0.55	3.4
35	75.99	3.22	High	Yes	-5.74	0.55	2.73
42	57.53	1.98	High	Yes	-5.32	0.58	2.42
44	57.53	2.23	High	Yes	-5.33	0.57	2.46

Figure 9. Metabolism and absorption of key antioxidant esters and ketones of selected phenolic acids.

4. Discussion

As the principal regulator of the redox homeostasis in cells, the cap ‘n’ collar basic leucine zipper (CNC-bZip) transcription factor, Nrf2 counterpoises the free radical production and maintains cellular redox homeostasis [47]. Depleted Nrf2, due to oxidative stress, senescence, or epigenetic suppression, drives the accumulation of free radicals in cells, lead-

ing to a pathogenic state. Since the discovery of Nrf2 in the 1990s, its physiological spectrum has expanded extensively [7,33,48,49]. Currently, there are several botanicals and dietary supplements in the market with Nrf2-activation claim; however, only one FDA-approved Nrf2 activator, Tecfidera (dimethylfumarate), for the treatment of multiple sclerosis can be recognized [50]. Therefore, the design and development of Nrf2-based therapeutics to mitigate oxidative stress-associated diseases remain a much-needed area of study.

Phenolic acids are among the vital antioxidant metabolites of a plant-based diet with the ability to activate the Nrf2 pathway [51]. Numerous studies indicate the antioxidant and other pharmacological properties of these plant secondary metabolites [8,51]. Caffeic acid, a vital antioxidant phenolic acid has been studied for more than 65 years [52,53]. Initially identified as a fungistatic agent, it was found to be a bioavailable and rapidly metabolized bioactive compound [52,54,55]. The synthesis of its esters began in the 1950s as well and continues to date for more potent versions of the parent molecule [56]. Other phenolic acids used in this study *viz.* hydro caffeic acid, ferulic, and gallic acid have also been well studied for more than 60 years and numerous analogs are available [57–59]. However, owing to their clinical significance, efforts are continuously underway to develop their novel and potent analogs of phenolic acids and this effort holds practical significance. In line with our work on polyphenol analogs, we synthesized an array of phenolic acid analogs with variable amide and ester moieties and assessed their antioxidant activity *in situ*, in cells, and *D. melanogaster*. We found that these compounds exhibit antioxidant capacity and induce cellular antioxidant enzymes at basal conditions. Our study identified unique polyphenol analogs with a strong ability to scavenge free radicals and stimulate GPx in cells (Figures 1, 4 and 6). We also found that the cytoprotective impacts of phenolic acid amides and esters are possibly interceded by their coordinated Nrf2 and ERK receptor activity (Figures 7 and 8).

Our findings complement previous data on the pharmacological spectrum of phenolic acids and their derivatives. Esterification of caffeic acid leads to the enhancement of its antioxidant capacities [60]. Likewise, novel amides of caffeic acid improve cell survival and cytoprotection [61]. A similar impact on biological activity has been shown by amides and ketones of ferulic acid, gallic acid, and hydroxy ferulic acid [62–64]. These antioxidant activities of phenolic acid(s) and their derivatives transcend free radical mitigation and extend benefits in different disease states as well. Caffeic acid amides have shown cytoprotective potential by inhibiting β -amyloid fibrillization and cytotoxicity [65]. Similarly, gallic acid amides have shown the ability to inhibit α -synuclein, a protein involved in the pathogenesis of Parkinson's disease [66]. CAPE also protects neurons against cisplatin-induced neurotoxicity via activation of the AMPK/SIRT1 pathway [67]. However, we did not observe any significant increase in both SIRT1 (Figure S2) and AMPK (Figure S3) pathways by CAPE or other analogs. It might be attributed to treatment at the basal level and lack of oxidative stress. Apart from the neuroprotective spectrum, the pharmacological sphere of phenolic acid derivatives extends to infectious diseases as well. Esters and amides of ferulic and caffeic acid have shown the ability to inhibit HIV-1 reverse transcriptase [68,69]. Next, the recent literature suggests that ERK, a member of the mitogen-activated protein kinase (MAPK) family of serine/threonine protein kinases, plays a key role in cell survival and is essential for antioxidant response by polyphenols [70]. The cellular activation of ERK by the ketone **44** as an extracellular stimulus is similar to previous reports indicating ERK activation by phenolic acids and their derivatives [18,21,36,67]. As ERK also plays a central role in morphogenesis and physiological homeostasis of *Drosophila*, its probable activation by ketone **44** indicates organized functional changes and improved tissue homeostasis [71]. Further, on metabolic front our simulation showed that ketone **44** exhibited strongest metabolic uptake among the analyzed polyphenol analogs. This supports the potent *in vivo* activity of ketone **44** in *Drosophila*.

This study demonstrates that the antioxidant effect of phenolic acids does not only depend on the presence of the catechol moiety. Interestingly, the replacement of the carboxylic acid functional group by the ketone function increases the antioxidant effect of

the molecule. Unlike the ketone analog, the amide and ether analogs were less active. The effect of ketone **44** can be attributed to the favorable interactions as predicted by molecular docking. Increased lipophilicity is probably an important factor to consider since ketone **44** is three times more lipophilic than caffeic acid. Compared to CAPE, ketone **44** is more stable since it is less conducive to hydrolysis. Investigations of the position of the 3,4-dihydroxyls of ketone **44** may have an effect on its activity. These arguments agree with a recent study in which the amide derivative of CAPE was ineffective against antioxidant transcription factors [72]. Di-hydroxylated analogs at 2,5 positions have demonstrated interesting anti-cancer effects [32,72]. The effect of increased lipophilicity, as well as the presence of the unsaturated α - β unsaturated ketone versus a simple ketone, can be as important.

Our study shows mechanisms underlying the antioxidant potential of selected phenolic acids; however, several future investigations can be suggested. Activation of the Nrf2 pathway is dependent on the endogenous inhibitor of Nrf2, Keap1, function as an evolutionarily conserved intracellular defense mechanism to counteract oxidative stress [47,73]. Moreover, activation of antioxidant enzymes depends on the spatial distribution of both Nrf2 and Keap1 [48]. Therefore, future experiments can be targeted to understand the impact of the novel phenolic acid derivatives on Keap1, the main intracellular regulator of Nrf2 activation. Interestingly, our pilot experiment did show the nuclear migration of Nrf2, thus, supporting further experiments on intricate cellular antioxidant mechanisms (Figure S4).

Most investigated Nrf2 activators function as non-specific covalent modification of thiol groups Keap1 cysteine residues. Owing to its potent antioxidant activity, we expect ketone **44** to inhibit Keap1-Nrf2 binding, leading to nuclear translocation of Nrf2 *in vitro* (Figure S5). The lack of comparative analysis of ketone **44** with small-molecule Nrf2 activators such as dimethylfumarate, curcumin, quercetin, and sulforaphane hinders a broader understanding of its efficacy. The novel compounds are also warranted investigations on their ability to induce epigenetic changes in histones, owing to Nrf2-ERK activation. It is vital to note that despite the lack of downstream SOD activation *in vivo* (Figure 6D), Nrf2 activation did result in increased HO-1 and GPx levels, indicating a SOD independent but wider antioxidant spectrum of the tested compounds *in vivo*. It is well known that certain polyphenols exhibit pro-oxidant activities at higher concentrations depending on the cellular microenvironment [74]. Therefore, the new derivatives of phenolic acids need to be further assessed for their safety using multiple-dose-dependent *in vitro* and *in vivo* systems. Further, it will be interesting to examine the anti-cancer effect of these phenolic acid derivatives in cancer cells and experimental animal models.

5. Conclusions

We adopt natural product supplementation as a strategy for managing oxidative stress-mediated pathophysiological conditions. The discovery of natural product inspired new Nrf2 activators and establishing their mechanism of action can be of great pharmacological value. We have shown that multiple esters and ketones of phenolic acids exhibit potent antioxidant activity and activate antioxidant enzymes such as GPx, and HO-1 via the Nrf2-ARE pathway. Importantly, selected derivatives of phenolic acids, which constitute the human diet, exhibit safe and non-toxic activity in cells. Further, Nrf2 activation of both parent molecules (CA and CAPE) and the derivatives, particularly analog **44** is ERK-dependent. The design of CAPE's analog series for the investigation of the effect of structural modifications on all parts of this molecule provided a clear picture. The effect of caffeic acid analogs, as well as CAPE, are not due only to the presence of the catechol moiety. Our experiments have identified ketone **44** as a novel activator of Nrf2 *in vivo* and in cells.

Supplementary Materials: The following supporting information can be downloaded at: <https://www.mdpi.com/article/10.3390/app12063062/s1>, Figure S1: Figures and tables showing detailed antioxidant activity and chemical characteristics of Caffeic acid and CAPE analogs (100 μ M) as measured using ABTS, FRAP, and ORAC antioxidant assays; Figure S2: The impact of Caffeic acid and CAPE analogs on cytochrome C levels as the toxicity indicator. WI-38 cells were pre-treated

with 10 μM of the selected compounds for 24 h and then the cytochrome C levels were measured using ELISA; Figure S3: The impact of Caffeic acid and CAPE analogs on SIRT1 levels. 293T cells were pre-treated with 10 μM of the selected compounds for 24 h and then the selected biomarkers were observed using western blot; Figure S4: The impact of Caffeic acid and CAPE analogs on Nrf2 pathway activation. 293T cells were pre-treated with 10 μM of the selected compounds for 24 h and then the protein and RNA were extracted using RIPA buffer and TRIZOL. (A-B) mRNA increase in HO-1 and (C) validation of p-NRF2 by analog 44. Ordinary one-way analysis of variance (ANOVA) was performed followed by Dunnett's multiple comparisons test to identify statistical difference ** $p < 0.01$, **** $p < 0.0001$; Figure S5: The subcellular localization of Nrf2 following treatment with compound 44, the ketone analog of CAPE. 293T cells were pre-treated with 10 μM of the compound 44 for 24 h and then the nuclear protein was extracted, and immunoblotting was performed; Additional Supplementary Material: NMR data.

Author Contributions: K.S.B.: Conceptualization, Investigation, Data curation, Writing—original draft, and updated versions. M.A.N.: Investigation, Data curation, Writing—original draft, and updated versions. K.M.E.: Supervision, Writing—original draft & updated versions, corrections and editing. J.A.D.: Investigation and Data curation. L.M.L.: Investigation and Data curation. G.L.-C.: Investigation and Data curation. M.S.: Investigation, Resources, and Manuscript Revision. F.S.A.: Manuscript Revision. M.T. and H.P.V.R.: Supervision, Funding, Writing—original draft & updated versions, corrections and editing. All authors have read and agreed to the published version of the manuscript.

Funding: M.T. and H.P.V.R. acknowledge funding from the Discovery Grant of the Natural Sciences and Engineering Research Council (NSERC) of Canada. M.T. also received funds from New Brunswick Innovation Foundation.

Data Availability Statement: Available on request from the corresponding author.

Acknowledgments: The authors thank Evan Kerek and Basil P. Hubbard for their help with western blots, cell culture, RNA extraction, and providing other resources. Anthony Galenza and Edan Foley for their help with fly study and qPCR, and Aja Rieger and Sabina Baghirova for help with flow cytometry analysis. The authors also thank Katie Chen for her help with the cell fractionation experiment. Special thanks to Basil P. Hubbard, Hasan Uludag, Mohamed Salla, and Danny Galleguillos for providing antibodies, HEK293T cells, and valuable suggestions for this study.

Conflicts of Interest: The authors declare no conflict of interest.

References

1. Harman, D. Aging: A theory based on free radical and radiation chemistry. *Sci. Aging Knowl.* **2002**, *2002*, 14. [[CrossRef](#)]
2. Mills, G.C. Hemoglobin catabolism: I. Glutathione peroxidase, an erythrocyte enzyme which protects hemoglobin from oxidative breakdown. *J. Biol. Chem.* **1957**, *229*, 189–197. [[CrossRef](#)]
3. McCord, J.M.; Fridovich, I. Superoxide dismutase: An enzymic function for erythrocuprein (hemocuprein). *J. Biol. Chem.* **1969**, *244*, 6049–6055. [[CrossRef](#)]
4. Miquel, J.; Economos, A.; Fleming, J.; Johnson, J., Jr. Mitochondrial role in cell aging. *Exp. Gerontol.* **1980**, *15*, 575–591. [[CrossRef](#)]
5. Sies, H. 1-Oxidative Stress: Introductory Remarks. In *Oxidative Stress*; Academic Press: London, UK, 1985; pp. 1–8.
6. Phaniendra, A.; Jestadi, D.B.; Periyasamy, L. Free radicals: Properties, sources, targets, and their implication in various diseases. *Indian J. Clin. Biochem.* **2015**, *30*, 11–26. [[CrossRef](#)] [[PubMed](#)]
7. Bhullar, K.S.; Rupasinghe, H. Polyphenols: Multipotent therapeutic agents in neurodegenerative diseases. *Oxidative Med. Cell. Longev.* **2013**, *2013*, 891748. [[CrossRef](#)]
8. Croft, K.D. Dietary polyphenols: Antioxidants or not? *Arch. Biochem. Biophys.* **2016**, *595*, 120–124. [[CrossRef](#)]
9. Tsao, R. Chemistry and biochemistry of dietary polyphenols. *Nutrients* **2010**, *2*, 1231–1246. [[CrossRef](#)] [[PubMed](#)]
10. Li, Z.; Moalin, M.; Zhang, M.; Vervoort, L.; Mommers, A.; Haenen, G.R. Delocalization of the Unpaired Electron in the Quercetin Radical: Comparison of Experimental ESR Data with DFT Calculations. *Int. J. Mol. Sci.* **2020**, *21*, 2033. [[CrossRef](#)] [[PubMed](#)]
11. Sies, H. Total antioxidant capacity: Appraisal of a concept. *J. Nutr.* **2007**, *137*, 1493–1495. [[CrossRef](#)]
12. Forman, H.J.; Davies, K.J.; Ursini, F. How do nutritional antioxidants really work: Nucleophilic tone and para-hormesis versus free radical scavenging in vivo. *Free Radic. Biol. Med.* **2014**, *66*, 24–35. [[CrossRef](#)] [[PubMed](#)]
13. Tu, T.; Giblin, D.; Gross, M.L. Structural determinant of chemical reactivity and potential health effects of quinones from natural products. *Chem. Res. Toxicol.* **2011**, *24*, 1527–1539. [[CrossRef](#)]
14. L Suraweera, T.; Rupasinghe, H.; Dellaire, G.; Xu, Z. Regulation of Nrf2/ARE pathway by dietary flavonoids: A friend or foe for cancer management? *Antioxidants* **2020**, *9*, 973. [[CrossRef](#)] [[PubMed](#)]

15. Labunskyy, V.M.; Hatfield, D.L.; Gladyshev, V.N. Selenoproteins: Molecular pathways and physiological roles. *Physiol. Rev.* **2014**, *94*, 739–777. [[CrossRef](#)] [[PubMed](#)]
16. Liang, L.; Gao, C.; Luo, M.; Wang, W.; Zhao, C.; Zu, Y.; Efferth, T.; Fu, Y. Dihydroquercetin (DHQ) induced HO-1 and NQO1 expression against oxidative stress through the Nrf2-dependent antioxidant pathway. *J. Agric. Food Chem.* **2013**, *61*, 2755–2761. [[CrossRef](#)]
17. Lee, D.-S.; Kim, K.-S.; Ko, W.; Li, B.; Jeong, G.-S.; Jang, J.-H.; Oh, H.; Kim, Y.-C. The cytoprotective effect of sulfuretin against tert-butyl hydroperoxide-induced hepatotoxicity through Nrf2/ARE and JNK/ERK MAPK-mediated heme oxygenase-1 expression. *Int. J. Mol. Sci.* **2014**, *15*, 8863–8877. [[CrossRef](#)]
18. Ma, J.-Q.; Ding, J.; Xiao, Z.-H.; Liu, C.-M. Puerarin ameliorates carbon tetrachloride-induced oxidative DNA damage and inflammation in mouse kidney through ERK/Nrf2/ARE pathway. *Food Chem. Toxicol.* **2014**, *71*, 264–271. [[CrossRef](#)] [[PubMed](#)]
19. Wruck, C.; Claussen, M.; Fuhrmann, G.; Römer, L.; Schulz, A.; Pufe, T.; Waetzig, V.; Peipp, M.; Herdegen, T.; Götz, M. Luteolin protects rat PC 12 and C6 cells against MPP+ induced toxicity via an ERK dependent Keap1-Nrf2-ARE pathway. In *Neuropsychiatric Disorders an Integrative Approach*; Springer: Vienna, Austria, 2007; pp. 57–67.
20. Wu, H.; Zhao, J.; Chen, M.; Wang, H.; Yao, Q.; Fan, J.; Zhang, M. The anti-aging effect of erythropoietin via the ERK/Nrf2-ARE pathway in aging rats. *J. Mol. Neurosci.* **2017**, *61*, 449–458. [[CrossRef](#)]
21. Feng, R.-B.; Wang, Y.; He, C.; Yang, Y.; Wan, J.-B. Gallic acid, a natural polyphenol, protects against tert-butyl hydroperoxide-induced hepatotoxicity by activating ERK-Nrf2-Keap1-mediated antioxidative response. *Food Chem. Toxicol.* **2018**, *119*, 479–488. [[CrossRef](#)]
22. Kassab, R.B.; Lokman, M.S.; Daabo, H.M.; Gaber, D.A.; Habotta, O.A.; Hafez, M.M.; Zhery, A.S.; Moneim, A.E.A.; Fouda, M.S. Ferulic acid influences Nrf2 activation to restore testicular tissue from cadmium-induced oxidative challenge, inflammation, and apoptosis in rats. *J. Food Biochem.* **2020**, *44*, e13505. [[CrossRef](#)] [[PubMed](#)]
23. Morroni, F.; Sita, G.; Graziosi, A.; Turrini, E.; Fimognari, C.; Tarozzi, A.; Hrelia, P. Neuroprotective effect of caffeic acid phenethyl ester in a mouse model of Alzheimer’s disease involves Nrf2/HO-1 pathway. *Aging Dis.* **2018**, *9*, 605. [[CrossRef](#)]
24. Romana-Souza, B.; Dos Santos, J.S.; Monte-Alto-Costa, A. Caffeic acid phenethyl ester promotes wound healing of mice pressure ulcers affecting NF- κ B, NOS2 and NRF2 expression. *Life Sci.* **2018**, *207*, 158–165. [[CrossRef](#)] [[PubMed](#)]
25. Zhou, D.; Yang, Q.; Tian, T.; Chang, Y.; Li, Y.; Duan, L.-R.; Li, H.; Wang, S.-W. Gastroprotective effect of gallic acid against ethanol-induced gastric ulcer in rats: Involvement of the Nrf2/HO-1 signaling and anti-apoptosis role. *Biomed. Pharmacother.* **2020**, *126*, 110075. [[CrossRef](#)] [[PubMed](#)]
26. Bhullar, K.S.; Lassalle-Claux, G.; Touaibia, M.; Rupasinghe, H.V. Antihypertensive effect of caffeic acid and its analogs through dual renin–angiotensin–aldosterone system inhibition. *Eur. J. Pharmacol.* **2014**, *730*, 125–132. [[CrossRef](#)] [[PubMed](#)]
27. Boudreau, L.H.; Maillet, J.; LeBlanc, L.M.; Jean-François, J.; Touaibia, M.; Flamand, N.; Surette, M.E. Caffeic acid phenethyl ester and its amide analogue are potent inhibitors of leukotriene biosynthesis in human polymorphonuclear leukocytes. *PLoS ONE* **2012**, *7*, e31833. [[CrossRef](#)]
28. Doiron, J.A.; Leblanc, L.M.; Hébert, M.J.; Levesque, N.A.; Paré, A.F.; Jean-François, J.; Cormier, M.; Surette, M.E.; Touaibia, M. Structure–activity relationship of caffeic acid phenethyl ester analogs as new 5-lipoxygenase inhibitors. *Chem. Biol. Drug Des.* **2017**, *89*, 514–528. [[CrossRef](#)] [[PubMed](#)]
29. LeBlanc, L.M.; Paré, A.F.; Jean-François, J.; Hébert, M.J.; Surette, M.E.; Touaibia, M. Synthesis and antiradical/antioxidant activities of caffeic acid phenethyl ester and its related propionic, acetic, and benzoic acid analogues. *Molecules* **2012**, *17*, 14637–14650. [[CrossRef](#)] [[PubMed](#)]
30. Sanderson, J.T.; Clabault, H.; Patton, C.; Lassalle-Claux, G.; Jean-François, J.; Paré, A.F.; Hébert, M.J.; Surette, M.E.; Touaibia, M. Antiproliferative, antiandrogenic and cytotoxic effects of novel caffeic acid derivatives in LNCaP human androgen-dependent prostate cancer cells. *Bioorg. Med. Chem.* **2013**, *21*, 7182–7193. [[CrossRef](#)]
31. Touaibia, M.; Surette, M.E. Modulators of Lipoxygenase and Cyclooxygenase Enzyme Activity. U.S. Patent Application No. 16/081,738, 25 April 2019.
32. Selka, A.; Doiron, J.A.; Lyons, P.; Dastous, S.; Chiasson, A.; Cormier, M.; Turcotte, S.; Surette, M.E.; Touaibia, M. Discovery of a novel 2, 5-dihydroxycinnamic acid-based 5-lipoxygenase inhibitor that induces apoptosis and may impair autophagic flux in RCC4 renal cancer cells. *Eur. J. Med. Chem.* **2019**, *179*, 347–357. [[CrossRef](#)] [[PubMed](#)]
33. Bhullar, K.S.; Jha, A.; Youssef, D.; Rupasinghe, H. Curcumin and its carbocyclic analogs: Structure-activity in relation to antioxidant and selected biological properties. *Molecules* **2013**, *18*, 5389–5404. [[CrossRef](#)]
34. Floegel, A.; Kim, D.-O.; Chung, S.-J.; Koo, S.I.; Chun, O.K. Comparison of ABTS/DPPH assays to measure antioxidant capacity in popular antioxidant-rich US foods. *J. Food Compos. Anal.* **2011**, *24*, 1043–1048. [[CrossRef](#)]
35. Magwere, T.; Chapman, T.; Partridge, L. Sex differences in the effect of dietary restriction on life span and mortality rates in female and male *Drosophila melanogaster*. *J. Gerontol. Ser. A Biol. Sci. Med. Sci.* **2004**, *59*, B3–B9. [[CrossRef](#)] [[PubMed](#)]
36. Yang, G.; Fu, Y.; Malakhova, M.; Kurinov, I.; Zhu, F.; Yao, K.; Li, H.; Chen, H.; Li, W.; Sheng, Y. Caffeic acid directly targets ERK1/2 to attenuate solar UV-induced skin carcinogenesis. *Cancer Prev. Res.* **2014**, *7*, 1056–1066. [[CrossRef](#)] [[PubMed](#)]
37. Sastry, G.M.; Adzhigirey, M.; Day, T.; Annabhimoju, R.; Sherman, W. Protein and ligand preparation: Parameters, protocols, and influence on virtual screening enrichments. *J. Comput.-Aided Mol. Des.* **2013**, *27*, 221–234. [[CrossRef](#)] [[PubMed](#)]
38. Jacobson, M.P.; Friesner, R.A.; Xiang, Z.; Honig, B. On the role of the crystal environment in determining protein side-chain conformations. *J. Mol. Biol.* **2002**, *320*, 597–608. [[CrossRef](#)]

39. Jacobson, M.P.; Pincus, D.L.; Rapp, C.S.; Day, T.J.; Honig, B.; Shaw, D.E.; Friesner, R.A. A hierarchical approach to all-atom protein loop prediction. *Proteins Struct. Funct. Bioinform.* **2004**, *55*, 351–367. [[CrossRef](#)] [[PubMed](#)]
40. *Schrödinger Release 2020-1: Prime*, Schrödinger; LLC: New York, NY, USA, 2020.
41. Harder, E.; Damm, W.; Maple, J.; Wu, C.; Reboul, M.; Xiang, J.Y.; Wang, L.; Lupyan, D.; Dahlgren, M.K.; Knight, J.L. OPLS3: A force field providing broad coverage of drug-like small molecules and proteins. *J. Chem. Theory Comput.* **2016**, *12*, 281–296. [[CrossRef](#)]
42. *Schrödinger Release 2020-1: LigPrep*, Schrödinger; LLC: New York, NY, USA, 2020.
43. Friesner, R.A.; Banks, J.L.; Murphy, R.B.; Halgren, T.A.; Klicic, J.J.; Mainz, D.T.; Repasky, M.P.; Knoll, E.H.; Shelley, M.; Perry, J.K. Glide: A new approach for rapid, accurate docking and scoring. 1. Method and assessment of docking accuracy. *J. Med. Chem.* **2004**, *47*, 1739–1749. [[CrossRef](#)] [[PubMed](#)]
44. Friesner, R.A.; Murphy, R.B.; Repasky, M.P.; Frye, L.L.; Greenwood, J.R.; Halgren, T.A.; Sanschagrin, P.C.; Mainz, D.T. Extra precision glide: Docking and scoring incorporating a model of hydrophobic enclosure for protein–ligand complexes. *J. Med. Chem.* **2006**, *49*, 6177–6196. [[CrossRef](#)] [[PubMed](#)]
45. Halgren, T.A.; Murphy, R.B.; Friesner, R.A.; Beard, H.S.; Frye, L.L.; Pollard, W.T.; Banks, J.L. Glide: A new approach for rapid, accurate docking and scoring. 2. Enrichment factors in database screening. *J. Med. Chem.* **2004**, *47*, 1750–1759. [[CrossRef](#)] [[PubMed](#)]
46. Daina, A.; Michielin, O.; Zoete, V. SwissADME: A free web tool to evaluate pharmacokinetics, drug-likeness and medicinal chemistry friendliness of small molecules. *Sci. Rep.* **2017**, *7*, 1–13. [[CrossRef](#)] [[PubMed](#)]
47. Bellezza, I.; Giambanco, I.; Minelli, A.; Donato, R. Nrf2-Keap1 signaling in oxidative and reductive stress. *Biochim. Biophys. Acta -Mol. Cell Res.* **2018**, *1865*, 721–733. [[CrossRef](#)] [[PubMed](#)]
48. Jain, A.K.; Bloom, D.A.; Jaiswal, A.K. Nuclear import and export signals in control of Nrf2. *J. Biol. Chem.* **2017**, *292*, 2052. [[CrossRef](#)] [[PubMed](#)]
49. Moi, P.; Chan, K.; Asunis, I.; Cao, A.; Kan, Y.W. Isolation of NF-E2-related factor 2 (Nrf2), a NF-E2-like basic leucine zipper transcriptional activator that binds to the tandem NF-E2/AP1 repeat of the beta-globin locus control region. *Proc. Natl. Acad. Sci. USA* **1994**, *91*, 9926–9930. [[CrossRef](#)] [[PubMed](#)]
50. Brennan, M.S.; Patel, H.; Allaire, N.; Thai, A.; Cullen, P.; Ryan, S.; Lukashev, M.; Bista, P.; Huang, R.; Rhodes, K.J. Pharmacodynamics of dimethyl fumarate are tissue specific and involve NRF2-dependent and-independent mechanisms. *Antioxid. Redox Signal.* **2016**, *24*, 1058–1071. [[CrossRef](#)] [[PubMed](#)]
51. Ghasemzadeh, A.; Ghasemzadeh, N. Flavonoids and phenolic acids: Role and biochemical activity in plants and human. *J. Med. Plants Res.* **2011**, *5*, 6697–6703. [[CrossRef](#)]
52. Kuć, J.; Henze, R.; Ullstrup, A.; Quackenbush, F. Chlorogenic and Caffeic Acids as Fungistatic Agents Produced by Potatoes in Response to Inoculation with *Helminthosporium carbonium* 1, 2. *J. Am. Chem. Soc.* **1956**, *78*, 3123–3125. [[CrossRef](#)]
53. Sondheimer, E. On the distribution of caffeic acid and the chlorogenic acid isomers in plants. *Arch. Biochem. Biophys.* **1958**, *74*, 131–138. [[CrossRef](#)]
54. Booth, A.N.; Emerson, O.; Jones, F.T.; DeEds, F. Urinary metabolites of caffeic and chlorogenic acids. *J. Biol. Chem.* **1957**, *229*, 51–59. [[CrossRef](#)]
55. Broda, B.; Jaroniewski, W.; Swiatek, L. Occurrence of caffeic acid in some medicinal plants. *Acta Pol. Pharm.* **1960**, *17*, 301–306.
56. Tamura, S.; Ohkuma, K.; Hayasi, T. On the Antioxygenic Property of Caffeic and Dihydrocaffeic Esters. *J. Agric. Chem. Soc. Jpn.* **1952**, *26*, 410–412.
57. Bernhard, K.; Albrecht, H. Stoffwechselprodukte des Mikroorganismus *Phycomyces Blakesleeanus* in glucosehaltiger Nährlösung und Untersuchungen über das Wachstum dieses Schimmelpilzes bei verschiedenen Stickstoffquellen. *Helvetica Chim. Acta* **1947**, *30*, 627–632. [[CrossRef](#)] [[PubMed](#)]
58. Gortner, W.A.; Kent, M.J.; Sutherland, G. Ferulic and p-coumaric acids in pineapple tissue as modifiers of pineapple indoleacetic acid oxidase. *Nature* **1958**, *181*, 630–631. [[CrossRef](#)]
59. Neish, A. Preparation of caffeic and dihydrocaffeic acids by methods suitable for introduction of C14 into the β -position. *Can. J. Biochem. Physiol.* **1959**, *37*, 1431–1438. [[CrossRef](#)] [[PubMed](#)]
60. Zheng, Y.-Z.; Deng, G.; Guo, R.; Fu, Z.-M.; Chen, D.-F. Effects of different ester chains on the antioxidant activity of caffeic acid. *Bioorg. Chem.* **2020**, *105*, 104341. [[CrossRef](#)] [[PubMed](#)]
61. Moosavi, F.; Hosseini, R.; Rajaian, H.; Silva, T.; e Silva, D.M.; Saso, L.; Edraki, N.; Miri, R.; Borges, F.; Firuzi, O. Derivatives of caffeic acid, a natural antioxidant, as the basis for the discovery of novel nonpeptidic neurotrophic agents. *Bioorg. Med. Chem.* **2017**, *25*, 3235–3246. [[CrossRef](#)]
62. Kosuru, R.Y.; Roy, A.; Das, S.K.; Bera, S. Gallic acid and gallates in human health and disease: Do mitochondria hold the key to success? *Mol. Nutr. Food Res.* **2018**, *62*, 1700699. [[CrossRef](#)]
63. Michels, B.; Zwaka, H.; Bartels, R.; Lushchak, O.; Franke, K.; Endres, T.; Fendt, M.; Song, I.; Bakr, M.; Budragchaa, T. Memory enhancement by ferulic acid ester across species. *Sci. Adv.* **2018**, *4*, eaat6994. [[CrossRef](#)]
64. Sidoryk, K.; Jaromin, A.; Filipczak, N.; Cmoch, P.; Cybulski, M. Synthesis and antioxidant activity of caffeic acid derivatives. *Molecules* **2018**, *23*, 2199. [[CrossRef](#)] [[PubMed](#)]

65. Tu, L.-H.; Tseng, N.-H.; Tsai, Y.-R.; Lin, T.-W.; Lo, Y.-W.; Charng, J.-L.; Hsu, H.-T.; Chen, Y.-S.; Chen, R.-J.; Wu, Y.-T. Rationally designed divalent caffeic amides inhibit amyloid- β fibrillization, induce fibril dissociation, and ameliorate cytotoxicity. *Eur. J. Med. Chem.* **2018**, *158*, 393–404. [[CrossRef](#)] [[PubMed](#)]
66. Chen, L.; Huang, G.-L.; Lü, M.-H.; Zhang, Y.-X.; Xu, J.; Bai, S.-P. Amide derivatives of Gallic acid: Design, synthesis and evaluation of inhibitory activities against in vitro α -synuclein aggregation. *Bioorg. Med. Chem.* **2020**, *28*, 115596. [[CrossRef](#)] [[PubMed](#)]
67. Ferreira, R.S.; Dos Santos, N.A.G.; Bernardes, C.P.; Sisti, F.M.; Amaral, L.; Fontana, A.C.; Dos Santos, A.C. Caffeic acid phenethyl ester (CAPE) protects PC12 cells against cisplatin-induced neurotoxicity by activating the AMPK/SIRT1, MAPK/Erk, and PI3k/Akt signaling pathways. *Neurotox. Res.* **2019**, *36*, 175–192. [[CrossRef](#)] [[PubMed](#)]
68. Fesen, M.R.; Pommier, Y.; Leteurtre, F.; Hiroguchi, S.; Yung, J.; Kohn, K.W. Inhibition of HIV-1 integrase by flavones, caffeic acid phenethyl ester (CAPE) and related compounds. *Biochem. Pharmacol.* **1994**, *48*, 595–608. [[CrossRef](#)]
69. Sonar, V.P.; Corona, A.; Distinto, S.; Maccioni, E.; Meleddu, R.; Fois, B.; Floris, C.; Malpure, N.V.; Alcaro, S.; Tramontano, E. Natural product-inspired esters and amides of ferulic and caffeic acid as dual inhibitors of HIV-1 reverse transcriptase. *Eur. J. Med. Chem.* **2017**, *130*, 248–260. [[CrossRef](#)] [[PubMed](#)]
70. Farzaei, M.H.; Tewari, D.; Momtaz, S.; Argüelles, S.; Nabavi, S.M. Targeting ERK signaling pathway by polyphenols as novel therapeutic strategy for neurodegeneration. *Food Chem. Toxicol.* **2018**, *120*, 183–195. [[CrossRef](#)] [[PubMed](#)]
71. Hayashi, S.; Ogura, Y. ERK signaling dynamics in the morphogenesis and homeostasis of Drosophila. *Curr. Opin. Genet. Dev.* **2020**, *63*, 9–15. [[CrossRef](#)] [[PubMed](#)]
72. Murugesan, A.; Lassalle-Claux, G.; Hogan, L.; Vaillancourt, E.; Selka, A.; Luiker, K.; Kim, M.J.; Touaibia, M.; Reiman, T. Antimyeloma Potential of Caffeic Acid Phenethyl Ester and Its Analogues through Sp1 Mediated Downregulation of IKZF1-IRF4-MYC Axis. *J. Nat. Prod.* **2020**, *83*, 3526–3535. [[CrossRef](#)]
73. Niture, S.K.; Khatri, R.; Jaiswal, A.K. Regulation of Nrf2—An update. *Free Radic. Biol. Med.* **2014**, *66*, 36–44. [[CrossRef](#)]
74. Fernando, W.; Rupasinghe, H.V.; Hoskin, D.W. Dietary phytochemicals with anti-oxidant and pro-oxidant activities: A double-edged sword in relation to adjuvant chemotherapy and radiotherapy? *Cancer Lett.* **2019**, *452*, 168–177. [[CrossRef](#)]